CrossMark

ORIGINAL PAPER

A critical review of potential tsunamigenic sources as first step towards the tsunami hazard assessment for the Napoli Gulf (Southern Italy) highly populated area

I. Alberico[1] · **F. Budillon[1]** · **D. Casalbore[2]** · **V. Di Fiore[1]** · **R. Iavarone[3]**

Abstract Catastrophic tsunami events like those occurred in Papua New Guinea in 1998, Sumatra in 2004 and Japan in 2011, attracted the attention of the scientific community and promoted the development of different tools for assessing tsunami hazard. A preliminary step towards this goal is the knowledge of the events which might affect a specific coastal zone. In this context, we propose a method to identify the tsunami events possibly occurring in areas characterized by scarce data and a non-conservative environment. Accordingly, we propose different indices to summarize the knowledge on tsunami triggering mechanisms (earthquakes, landslides, volcanic eruptions), the characteristics of those mechanisms (magnitude of earthquakes, volume of landslide, Volcanic Explosivity Index) and tsunami features (water height, run-up, wave amplitude, propagation time). This knowledge, considered over a wider area than that of interest, allows for a paramount vision of possible hazardous events that could affect a particular coastal zone. Moreover, the tsunami simulation data and the analysis of potentially tsunamigenic slides which occurred on the Campania continental margins were also considered in the analysis. We focused our attention on Napoli megacity, because the high population density (about 1 million of people live on a territory of 117 km^2), together with the presence of active volcanic areas (Ischia, Somma-Vesuvio and Campi Flegrei), make this city potentially exposed to tsunami risk. The main outcome of such an approach shows that in the near field a tsunami amplitude varying from a few centimetres (30–40 cm) to some metres (1–4 m) might be expected at the coastline if the tsunami event was triggered by volcanic

✉ I. Alberico
ines.alberico@iamc.cnr.it

[1] Istituto per l'Ambiente Marino Costiero, IAMC-CNR, Calata Porta di Massa, 80133 Naples, Italy

[2] Sapienza, Università di Roma, P.le Aldo Moro 5, 00185 Rome, Italy

[3] Istituto di Biologia Agroambientale e Forestale, IBAF-CNR, Via Pietro Castellino 111, 80131 Naples, Italy

activity, whereas no relevant tsunami event should be expected given the peculiar seis-micity of the Neapolitan volcanic areas, with earthquakes rarely exceeding 4 Mw, if any possible cascade effects are overlooked. A morphometric analysis of high-resolution bathymetry collected between Ventotene Island and the Gulf of Salerno has shown that the submarine southern sectors of the Ischia Island and the Sorrento Peninsula are charac-terized by a high density of landslide scars, being thus a potential source area of landslide-generated tsunamis. However, despite the susceptibility of these areas to recurrent slope failures, only four submarine landslide scars were found to be potentially tsunamigenic with estimated tsunami amplitude of few metres at the coastline as predicted by coupling slide morphometry with tsunami amplitude equations. Concerning the tsunamis generated by earthquakes in the Western Mediterranean, only those triggered by high magnitude events (value ≥ 6–7 Mw) might affect the city of Napoli with an amplitude not exceeding 0.5 m, in about 30′.

1 Introduction

The occurrence of tsunamis in different areas around the world and the intense urban-ization of the coastal zones (SOER 2015) drew the attention of the scientific community in the last decades. Scientists have been motivated to develop methodologies to trace the extension of areas possibly exposed to tsunami risk, as main step to the hazard assessment along the coasts.

Grezio et al. (2012) define the risk as Risk = Hazard × Exposed elements × Vulner-ability in accordance with the general definition of UNESCO (1972) and Fournier D'Albe (1979); this definition was adopted for evaluating several geophysical risks (Glade 2003; Pesaresi et al. 2007; Lirer et al. 2001, 2010). Hazard is the probability of occurrence of a dangerous event in a fixed future time. Exposure measures people, property, systems or other elements present in hazardous zones that are thereby subject to potential losses. Vulnerability is the proportion of lives or goods likely to be lost and accounts for the characteristics of a system or asset that make it susceptible to the damaging effects of a hazard (Alberico and Petrosino 2015).

The contouring of coastal zones potentially exposed to tsunami waves represents an important step towards the development of a system able to react and/or to cope with such an event (i.e. adaptive capacity and/or coping capacity). In the last decade, probabilistic and deterministic approaches were developed to assess the tsunami hazard taking advan-tage from computer systems.

The probabilistic method requires data on a significant number of events; therefore, it is a method used mainly for tsunami triggered by earthquakes. Relationships linking earth-quakes occurrence and tsunamis incidence were found to identify the probability rate of tsunamis (Tinti 1991a, b; Tinti and Gavagni 1995; Orfanogiannaki and Papadopoulos 2004; González et al. 2009). For tsunamis induced by slides or by volcanic activity, average recurrence times of the events are much more difficult to identify owing to the overall lack of data (Ward 2001). In this case, a deterministic approach (Tinti et al. 1999a, 2006a, 2011), possibly joined with the scenario concept, has to be invoked. The worst-case scenario and the multi-scenario (Papathoma and Dominey-Howes 2003; Tinti and Armigliato 2003; Tinti et al. 2008; Eckert et al. 2012; Omira et al. 2010; Nguyen et al.

2014; Dall'Osso et al. 2014; Alberico and Petrosino 2015) are the principal methods used to delineate the hazard zones. The former considers only the largest event occurred in the past, while the latter takes into consideration more events with different magnitudes.

In the present work, we have carried out a comprehensive analysis of potential and historical tsunamigenic events that might have struck the city of Napoli from near (from Venotene Gulf of Napoli to the Gulf of Salerno) and far (other Italian subregions and Western Mediterranean Sea) fields. The aim of the paper is to present a methodological approach useful to identify potential tsunamigenic sources as first step towards the tsunami hazard assessment in areas characterized by scarce data and a non-conservative environment as the Gulf of Napoli. Specifically, this approach consists in the integration of results coming from: (a) a critical review of tsunamigenic sources from the available tsunami database and scientific literatures; (b) the analysis of scientific literature concerning tsunami simulations in the Western Mediterranean Sea aimed at identifying the possible exposure of the study area to events generated in the far field; (c) the computation of the maximum tsunami amplitude that could be generated by submarine landslides through the coupling of scar morphometry with predictive tsunami amplitude equations (e.g. Watts 2000; McAdoo and Watts 2004; Rahiman and Pettinga 2006).

The main outcome of this integrated analysis is to point out the potential tsunamigenic sources and associated features that may affect the Gulf of Napoli, providing insights for a proper tsunami hazard assessment, a fundamental goal for scientific community and land-planners, mainly in consideration of the intense anthropization and tourist exploitation of this coastal sector.

2 Materials and method

The identification of tsunami events potentially hazardous for the city of Napoli outcomes from a multifaceted workflow, made up of four phases: (a) recovery and recording of data derived from available tsunami database and literature into tables, (b) data analysis, (c) rough assessment of tsunamigenic potential for submarine landslides, (d) summary of data. To better link the concept of potential hazard to the territory, the tsunami sources were grouped and analysed in far- and near-field events. The latter includes the events occurred in the Gulf of Napoli and in the adjacent areas (from Ventotene Island to the northern sector of the Gulf of Salerno), whereas the former the events occurred mostly in the Western and Central Mediterranean Sea.

In the first phase, the tsunami data available in scientific literature and EMTC database, for a time interval ranging between 2000 years B.C. to present, were collected (Fig. 1a). In addition, several extreme events out of this time interval were considered. The data were arranged into tables and managed in a Geographic Information System (GIS) framework, allowing to link all type of information to the geographical position of the tsunami source and to use the spatial analysis to draw maps.

In the second phase, five indices (Table 1), useful for the tsunami events classification, were evaluated for: (a) triggering mechanisms (earthquakes, volcanic eruptions, landslide) and exposed zones (subregion), (b) characteristics of the trigger mechanisms (earthquake magnitude, Volcanic Explosivity Index, volume range), (c) tsunami parameters (tsunami intensity). On this latter point, the scarcity of data prevented the identification of indices for other tsunami parameters (i.e. water height, run-up, tsunami amplitude and extension of inland inundation), so that their hazard potential was expressed with a value range,
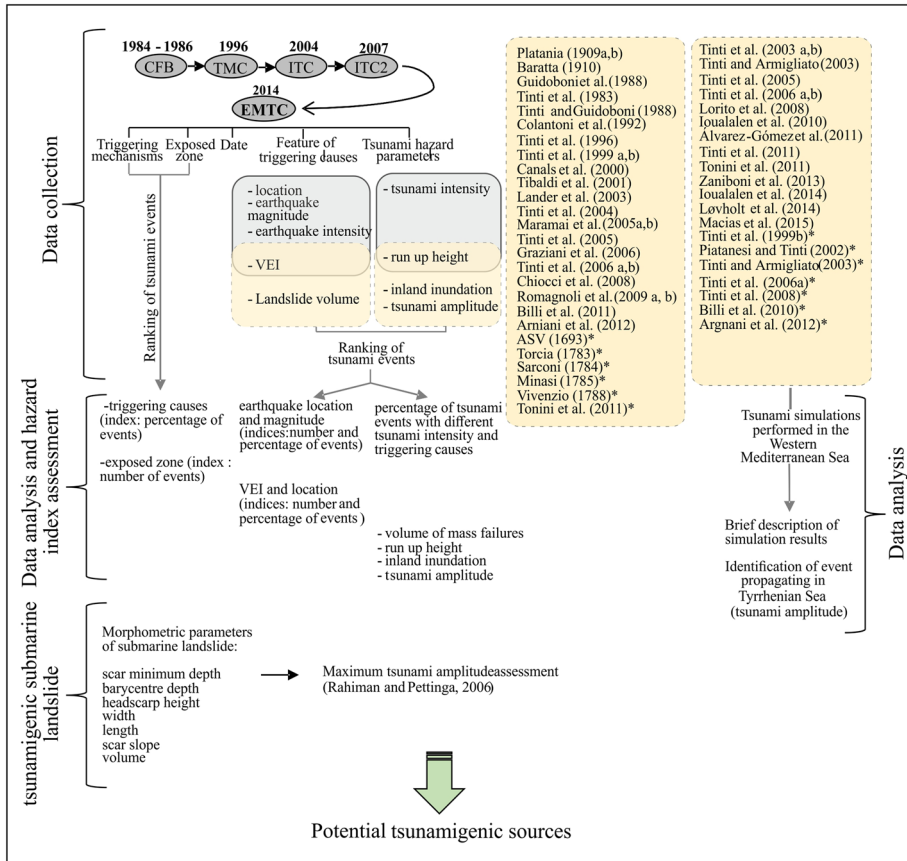
Fig. 1 Input data and associated sources used for the tsunami events valuation. The Italian Tsunami Catalogues (grey ellipses) and scientific works (yellow boxes) are the main source of triggering causes, exposed zones (subregion), time of occurrence, earthquake magnitude and tsunami intensity data. The data encircled in the pale yellow rectangle were collected from the scientific works reported in the coloured boxes on the right side of the image. Abbreviations meaning: CFB (Caputo and Faita Tsunami Catalogue, 1984 updated by Bedosti and Caputo in 1986), TMC (Tinti Maramai Catalogue; Tinti and Maramai 1996), ITC (Italia Tsunami Catalogue; Tinti et al. 2004), ITC2 (Italian Tsunami Catalogue Two; Tinti et al. 2007), EMTC (Euro-Mediterranean Tsunami Catalogue; Maramai et al. 2014)

identified from the analysis of 17 events, occurred mainly in the southern Italian subregions.

The index for the triggering mechanisms was calculated as the ratio of number of tsunamis triggered by a specific event (e.g. earthquakes) and the total number of tsunamis recorded into the GIS framework. For the feature of triggering mechanisms (e.g. earth-quake magnitude), the index was calculated as the ratio between the number of tsunamis pertaining to the single class of triggering mechanisms (e.g. earthquake magnitude values: unknown, 3.2–4.2, 4.2–5.2 etc.) and the total events with a specific triggering mechanisms. In the same way, the tsunami parameters (e.g. tsunami intensity) index was calculated.

Moreover, a brief description of tsunami simulations performed in the Western Mediterranean Sea and that could propagate in the Tyrrhenian Sea was made. For the

Table 1 Indicators and indices for triggering causes, subregion, earthquakes, magnitude, Volcanic Explosivity Index (VEI) and tsunami intensity are shown

Indicator	Index	Factors
Triggering mechanism	$\frac{N_i}{N_{tot}} \times 100$	N_i, number of tsunami events pertaining to each class of triggering mechanisms (earthquake inland, submarine earthquake, volcanic eruption, gravitational landslides, earthquake and landslide, eruption and landslides) N_{tot}, total number of tsunami events
Subregion	$\frac{N_{ic}}{N_{tot}} \times 100$	N_{ic}, number of tsunami events occurred in each subregion (Aeolian Islands, Apulia, Campania, Central Adriatic, Eastern Sicily, Gargano, Ionian Calabria, Latium, Liguria-Cote d'Azur, Messina Straits, North Adriatic, Northern Sicily, Sicily Channel, Tuscany, Tyrrhenian Calabria) also ranked by triggering mechanisms (earthquake inland, submarine earthquake, volcanic eruption, gravitational landslides, earthquake and landslide, eruption and landslides) N_{tot}, total number of tsunami events
Earthquake magnitude	$\frac{N_{ic}}{N_{tot\_e}} \times 100$	N_{ic}, number of tsunami events triggered by earthquake, ranked by both earthquake magnitude classes (3.2–4.2, 4.3–5.2, 5.3–6.2, 6.3–7.4) and earthquake source (inland, offshore) N_{tot_e}, total number of tsunami events triggered by earthquake
VEI	$\frac{N_{ic}}{N_{tot\_v}} \times 100$	N_{ic}, number of tsunami events triggered by volcanic eruption, ranked by both VEI (1, 2, 3, 4, 5) N_{tot_v}, total number of tsunami events triggered by volcanic eruption
Tsunami intensity	$\frac{N_{ic}}{N_{tot}} \times 100$	N_{ic}, number of tsunami events characterized by a specific level of intensity (2, 3, 4, 5, 6) and classified by triggering mechanisms (earthquake inland, submarine earthquake, volcanic eruption, gravitational landslides, earthquake and landslide, eruption and landslides) N_{tot}, total number of tsunami events

single simulation, the main feature of triggering causes, exposed zones and tsunami amplitude were summarized.

In the third phase, a simplified method coupling data on scar morphometry with predictive tsunami amplitude equations was used off the Latium and Campanian coastline, similarly to marine geo-hazard studies realized in other marine settings (Locat et al. 2004; Goldfinger et al. 2000; Bohannon and Gardner 2004; McAdoo and Watts 2004; Rahiman and Pettinga 2006; Casalbore et al. 2011, 2017; Casas et al. 2016). In detail, the analysis of high-resolution Digital Terrain Models obtained by swath bathymetric data (D'Argenio et al. 2004; Budillon et al. 2011a, b; Casalbore et al. 2014) was carried out to identify the morphometric parameters of the submarine mass failures identified in the near field. Those parameters are needed to assess the maximum tsunami amplitude (A) according to the equation of Rahiman and Pettinga (2006):

$$\lambda = 3.87(bd/\sin\sigma)^{0.5}$$
$$A = 0.224T[w/(w+\lambda)] \times \left[(\sin\sigma)^{1.29} - 0.746(\sin\sigma)^{2.29} + 0.170(\sin\sigma)^{3.29}\right](b/d)^{1.25} \quad (1)$$

where λ is the tsunami wavelength, b is the length of the scar along the slope, w is the width of the scar parallel to the slope, d is the water depth at the landslide barycentre, T is the head scarp height (assumed as a proxy of the maximum initial failure mass thickness normal to slope), and σ is the mean slope of failure scar. Moreover, to take into account the key role of the volumes of mass failure for the hazard assessment, only the landslide scars resulting from a unique mass-wasting event were considered in the analysis.

Despite the potential inaccuracy in using equations with parametric coefficients derived for a different part of the world and with different conditions, the equation was roughly calibrated on the basis of the computed maximum amplitude and observed run-up of tsunami waves generated by the tsunamigenic landslide occurred in 2002 in the relatively nearby Stromboli Island (Casalbore et al. 2011).

In the fourth phase, a summary of all data (e.g. indices, synthetic descriptions) was made to identify the potential tsunamigenic sources for the city of Napoli, associated with events occurred both in far- and near-fields.

3 Tsunami data analysis and hazard index

At the end of eighteenth century, tsunamis were included as secondary events in earthquakes (see Mallet 1854; Baratta 1901) or volcanic eruptions catalogues (Mercalli 1883; Baratta 1897). Since 1947, when a tsunami catalogue regarding all continents was published by Heck, several tsunami databases recording new detailed information were implemented (Fig. 1). The most recent database concerning the European-Mediterranean and Eastern Atlantic Regions (EMTC—Maramai et al. 2014) records 221 tsunamis in the Mediterranean Sea, whose 72 occurred in the M2 zone (Central Mediterranean Basin). The analysis of the events allowed us to define five indices expressing the dangerousness of tsunami sourcing in both far (Western Mediterranean Sea) and near (Gulf of Napoli and in the adjacent areas—from *Ventotene* Island to the northern sector of the Gulf of Salerno) fields with respect to the city of Napoli.
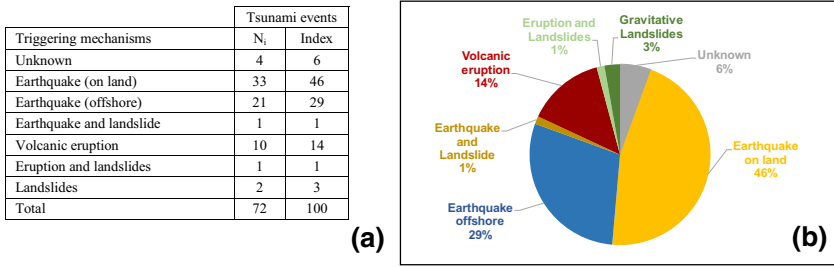
3.1 Triggering causes and subregions

According to the formula (1), the number of events (N_{ic}) and the percentage of triggering causes for the M2 zone were assessed. As reported in Fig. 2a, b, the tsunami events were triggered for the 75% by earthquakes, 14% by volcanic eruptions and 3% by both landslides and combined sources classes (Fig. 2a, b). The same indices, identified for each Italian subregion, highlight that the Campania, Liguria-Côte d'Azur, Aeolian Islands and Tyrrhenian Calabria coasts record the highest number of events, whereas the Latium subregion, the lowest one (Fig. 2c, d).

3.2 Characteristics of triggering events

The data analysis showed that earthquakes with magnitude > 5.3 Mw triggered a large number of tsunamis and even a different threshold of magnitude for the genesis of tsunamis occurs between earthquakes generated offshore and on land. The number of events (N_{ic}) concerning both the single class of earthquake magnitude and of tsunami source (in land and offshore) is reported in Fig. 3a, b.

The Volcanic Explosivity Index is known for the tsunamis triggered by volcanic eruptions; 7 out of 10 have a VEI ranging from 2 to 3. Similar to the earthquake magnitude index, the VEI data were used in the formula (1) to identify the index reported in Fig. 3c, d.

Triggering mechanisms	Tsunami events	
	N_i	Index
Unknown	4	6
Earthquake (on land)	33	46
Earthquake (offshore)	21	29
Earthquake and landslide	1	1
Volcanic eruption	10	14
Eruption and landslides	1	1
Landslides	2	3
Total	72	100

(a)

(b)

| Sub-region	Unknown		Earthquake (offshore)		Earthquake (on land)		Volcanic eruption		Landslide		Earthquake and landslide		Eruption and landslide		Total	
	N_{ic}	Index	N_{ic}	Index	N_{ic}	Index	N_{ic}	Index	N_{ic}	Index	N_{ic}	Index	N_{ic}	Index	N_{ic}	Index
Aeolian Islands		0.00	2	2.78		0.00	4	5.56	1	1.39		0.00	1	1.39	8	11.11
Apulia		0.00	1	1.39	1	1.39		0.00		0.00		0.00		0.00	2	2.78
Campania	2	2.78	1	1.39	2	2.78	5	6.94		0.00		0.00		0.00	10	13.89
Central Adriatic		0.00	2	2.78	2	2.78		0.00		0.00		0.00		0.00	4	5.56
Eastern Sicily		0.00	3	4.17	2	2.78	1	1.39		0.00		0.00		0.00	6	8.33
Gargano		0.00		0.00	2	2.78		0.00		0.00		0.00		0.00	2	2.78
Ionian Calabria		0.00	1	1.39	4	5.56		0.00		0.00		0.00		0.00	5	6.94
Latium		0.00		0.00	1	1.39		0.00		0.00		0.00		0.00	1	1.39
Liguria-Côte d'Azur	2	2.78	3	4.17	4	5.56		0.00		0.00		0.00		0.00	9	12.50
Messina Straits		0.00	3	4.17		0.00		0.00	1	1.39	1	1.39		0.00	5	6.94
North Adriatic		0.00		0.00	3	4.17		0.00		0.00		0.00		0.00	3	4.17
Northern Sicily		0.00	2	2.78	2	2.78		0.00		0.00		0.00		0.00	4	5.56
Sicily Channel		0.00	2	2.78		0.00		0.00		0.00		0.00		0.00	2	2.78
Tuscany		0.00		0.00	3	4.17		0.00		0.00		0.00		0.00	3	4.17
Tyrrhenian Calabria		0.00	1	1.39	7	9.72		0.00		0.00		0.00		0.00		11.11

(c)

(d)
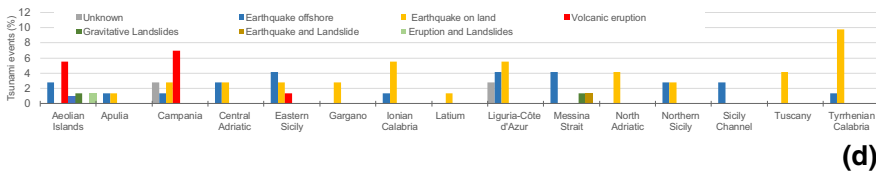
Fig. 2 Number and percentage of tsunami events classified for triggering causes (**a**) and graphic representation of tsunami percentage (**b**). The same type of data was reported for each Italian subregion in figures **c** and **d**

3.3 Tsunami parameters

The analysis of tsunami intensity pointed out that the greatest part of events (event percentage: 58%) has an intensity of 2, whereas only the 16% has an intensity higher than 3 (Fig. 4a). This parameter ranges from 2 to 4 for the events induced by volcanic eruptions, from 2 to 3 for those triggered by landslides, while a wider range varying from 2 to 6 characterizes the events triggered by earthquakes (Fig. 4b–f). For the latter, the highest percentage of tsunamis has an intensity of 2 and their percentage decreases of about three times for tsunami intensity of 3 and only 10 tsunamis have an intensity higher than 3 (Fig. 4b–f).

The analysis of field survey data retrieved from scientific papers, coupled with the information recorded into EMTC, pointed out that few information on tsunami parameters

Off shore	Earthquake magnitude	N_{ic}	Index
	Unknown	3	5.56
	3.2 - 4.2	3	5.56
	4.3 - 5.2	4	7.41
	5.3 - 6.2	8	14.81
	6.3 - 7.4	3	5.56
	Total	*21*	*38.89*

Inland	Earthquake magnitude	N_{ic}	Index
	Unknown	2	3.70
	3.2 - 4.2	1	1.85
	4.3 - 5.2	3	5.56
	5.3 - 6.2	13	24.07
	6.3 - 7.4	14	25.93
	Total	*33*	*61.11*

(a)

(b)

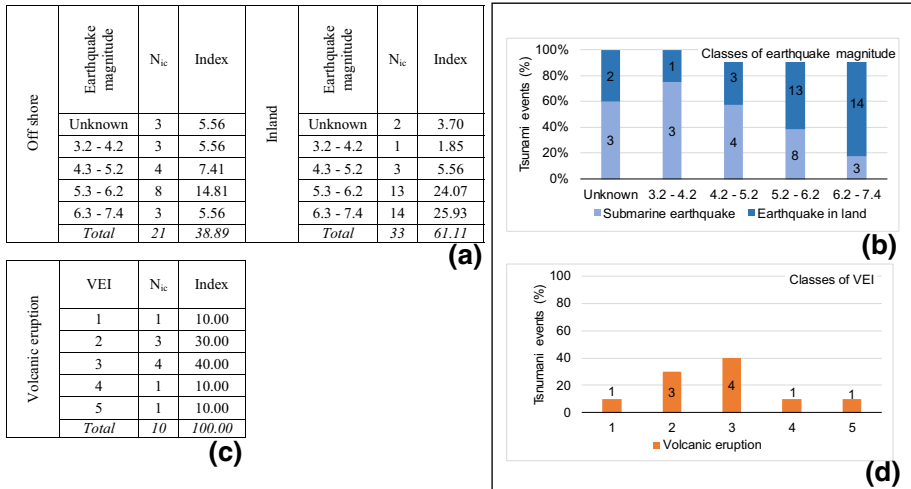| Volcanic eruption	VEI	N_{ic}	Index
	1	1	10.00
	2	3	30.00
	3	4	40.00
	4	1	10.00
	5	1	10.00
	Total	*10*	*100.00*

(c)

(d)

Fig. 3 The number of tsunamis and hazard index are reported for the single earthquake magnitude class and for source location (on land and offshore). These value was also plotted in the diagram "**b**". Similarly, the number and hazard index of tsunamis triggered by volcanic eruption was shown in figures "**c**" and "**d**", respectively

(water height, run-up, run down, inland inundation, wave amplitude, wave length, period, frequency) are available.

The tsunami amplitude, run-up and inland inundation parameters are often available only for few events. Moreover, these parameters are deeply conditioned by the local morphology of both sea floor and emerged area that prevent the assessment of experimental laws at regional scale (Szczucinski et al. 2006; Billi et al. 2010; Nakamura et al. 2012). Despite the paucity of information, we tried to summarize the available data in order to identify, for each parameter, the range of values to better constrain the hazard of tsunami events (Table 2a, b; for detail see online Appendix 1). The tsunami amplitude varies from 0.75 to 15 m, with the highest value characterizing the Eastern Sicily followed by Messina Straits and Aeolian Islands. The run-up ranges between 1 and 11.7 m, with the maximum value recorded in Messina Straits for the 1908 event. The inland inundation varies from 5 to 2400 m, with the maximum value still recorded in Messina Straits subregion.

4 Analysis of tsunami simulations performed in the Mediterranean Sea

The analysis of scientific literature concerning tsunami simulations aimed at identifying the possible exposure of the study area to events generated in the far field. The simulations of tsunami occurred in western Mediterranean Sea are widely described in Table 3, where the information on source area, main feature of triggering causes, exposed zones, tsunami amplitude and references is recorded. In contrast, we overlooked the tsunamis generated in the eastern Mediterranean Basin, because the Messina Strait acts as a barrier to their propagation in the Tyrrhenian Sea (Lorito et al. 2008).
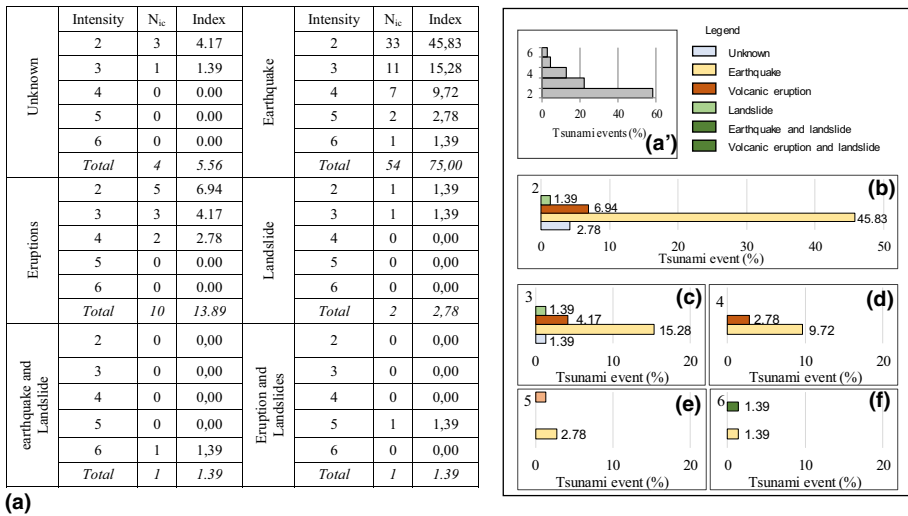
	Intensity	N_{ie}	Index		Intensity	N_{ie}	Index
Unknown	2	3	4.17	Earthquake	2	33	45,83
	3	1	1.39		3	11	15,28
	4	0	0.00		4	7	9,72
	5	0	0.00		5	2	2,78
	6	0	0.00		6	1	1,39
	Total	4	5.56		Total	54	75,00
Eruptions	2	5	6.94	Landslide	2	1	1,39
	3	3	4.17		3	1	1,39
	4	2	2.78		4	0	0,00
	5	0	0.00		5	0	0,00
	6	0	0.00		6	0	0,00
	Total	10	13.89		Total	2	2,78
earthquake and Landslide	2	0	0,00	Eruption and Landslides	2	0	0,00
	3	0	0,00		3	0	0,00
	4	0	0,00		4	0	0,00
	5	0	0,00		5	1	1,39
	6	1	1,39		6	0	0,00
	Total	1	1,39		Total	1	1,39

(a)

Fig. 4 The number of tsunamis events and hazard index are reported for each tsunami intensity classes and triggering causes (**a**). The figure "**a**" illustrates the percentage of tsunamis grouped only for intensity, while the figures from "**b**" to "**f**" point out, for the single tsunami intensity classes, the percentage of tsunami events classified for triggering causes

4.1 Tsunami generated by earthquakes

The geodynamic setting of Western Mediterranean basin is characterized by seismogenic faulting zones, as the Tell-Atlas thrust belt, the Southern Tyrrhenian thrust belt and the Eastern Sicily, able to generate earthquake-generated tsunamis that can pose significant hazard for the Mediterranean coasts (Fig. 5) (Tinti et al. 2005, 2011; Lorito et al. 2008; Sahal et al. 2009). Seven simulations of tsunamis triggered by earthquakes are reviewed and summarized in Table 3; they concerned the events occurred: (a) on 21 May 2003 (performed by Tinti et al. 2005), and on 10 October 1980 (simulated by Lorito et al. 2008) for the Algeria-Tunisia zone; (b) on 5 March 1823 along the offshore seismic belt (simulated by Lorito et al. 2008) in the Southern Tyrrhenian zone; (c) on 11 January 1693 (Tinti et al. 2005; Tonini et al. 2011) for the Eastern Sicily (Fig. 5). This latter event was possibly generated offshore, according to Tinti et al. (2001) and was located along the Hyblaean-Malta escarpment by Tinti and Armigliato (2003). However, Tonini et al. (2011) speculate that this event was related to a submarine landslide (volume = 4.1×10^9 m³; Argnani et al. 2012) along the Malta escarpment, which took place in waters deeper than 1800 m, triggered by a non-tsunamigenic earthquake occurred on the mainland. Tonini et al. (2011) also simulated the tsunami triggered by the strong earthquake occurred in the Messina Straits on 28 December 1908.

In the westernmost Mediterranean area, the Alboran Ridge is the only zone able to generate earthquake induced tsunamis. For this area, the results of several simulated events (Álvarez-Gómez et al. 2011) generated by earthquakes with magnitude ranging between 6 and 7 are reported in Table 3. In addition, Ioualalen et al. (2014) pointed out that the earthquakes sourcing on the French–Italian Riviera are recurrent but only strong earthquakes, such as the event occurred on 23 February 1887, could induce tsunamis (Table 2b).

Table 2 Summary of data for tsunami events affecting the Italian subregions retrieved from EMTC database and scientific literature. They were grouped in three sections: the triggering causes, features of triggering causes, tsunami features. In addition, the events providing data on tsunami features are listed in (b) (for detail on single event see the online Appendix 1)

		Classes	Details							Note
Triggering mechanisms		Earthquakes (75%)								
		Volcanic eruptions (14%)								
		Mass failures (3%)								
		More than one causes (3%)								
Features of triggering mechanisms		Earthquake magnitude ranging 3.2 - 7.9 Mw	Earthquakes offshore (11 events)	Magnitude range between 5.3 and 7.4 Mw						
			Earthquakes inland (27 events)	Magnitude range between 5.3 and 7.4 Mw						
			11 events	Magnitude lower than 5.3 Mw						
		VEI ranging from 1 to 5								
		Mass failure	Mass failure on land	Volume = 20×10⁶ m³ / 4-9×10⁶ m³						December 2002 - Aeolian Islands (Stromboli, Sciara del Fuoco).
				Volume = 0.2x10⁶ m³						April 1988 - Aeolian Islands (Vulcano, La Fossa)
				Volume = 2 km³ / 1 km³ / 0.52–0.95 km³						13 ka BP - Aeolian Islands (Stromboli) / 5.6 ka BP / 5 ka BP
			Mass failure offshore	Volume = 0.00219 km³ in shallow water / 0.0622 km³ (mean depth =800 m)						October 1979 Ligurian Sea (Nice airport)

Tsunami features	Tsunami intensity	ranging from 2 to 6	intensity = 2	number of events=42						Intensity ranges from: 2 to 4 for volcanic eruptions 2 to 3 for landslide 2 to 6 for earthquakes. Only 9 tsunami events have an intensity higher than 3.
			intensity = 3	number of events=16						
			intensity > 3 and ≤ 6	number of events=14						

	Tsunami amplitude	ranging from 0.75 to 16.0 m		≤2	>2 and ≤4	>4 and ≤6	>6 and ≤8	>8 and ≤10	>10	Total events with tsunami amplitude data = 9
			Earthquake		1		1			
			Volcanic eruption		2					
			Landslide	5	1	1	2		1	
			Volcanic eruption and earthquake							
			Earthquake and landslide						1	
			Volcanic eruption and landslide	4	1			1		

	Run up	ranging from 0.50 to 13.0 m		≤2	>2 and ≤4	>4 and ≤6	>6 and ≤8	>8 and ≤10	>10	Total events with run up data = 9
			Earthquake	1	1	1				
			Volcanic eruption		1					
			Landslide	2		2	1		3	
			Volcanic eruption and earthquake					1		
			Earthquake and landslide	3	1	5	3	3	1	
			Volcanic eruption and landslide	2	3	4	3	4	1	

	Inland inundation	range 5 - 2414 m		≤40	>40 - ≤80	>80 - ≤120	>120 - ≤160	>160 - ≤200	>200	Total events with inland inundation data = 10
			Earthquake	3						
			Volcanic eruption					1	2	
			Landslide						1	
			Volcanic eruption and earthquake	1						
			Earthquake and landslide	2	2	2		2	2	
			Volcanic eruption and landslide	10	8		1			

(a)

Date	Sub-region	Tsunami intensity	Tsunami amplitude (m)	Inland inundation (m)	Run-up height (m)	Mass failure (m³)
30 July 1627	Gargano	5	2.5		2.0-3.0	
14 April 1672	Central Adriatic	2		6.1		
11 January 1693	Eastern Sicily	5	15.0			
06 February 1783	Messina Straits	6	16.0	40.0 - 2.414.0	3.5 - 8.3	
25 April 1836	Ionian Calabria	4		12.19		
23 February 1887	Liguria-Côte d'Azur	3			1.5	
08 September 1905	Tyrrhenian Calabria	4			6.0	
23 October 1907	Ionian Calabria	3		30.0		
28 December 1908	Messina Straits	6	0.9 - 10.0	200.0 - 700.0	1.4 – 13.0	
03 July 1916	Aeolian Islands	2		20.0	10	
22 May 1919	Aeolian Islands	3		150.0 - 300.0		
11 September 1930	Aeolian Islands	4	2.0 - 3.0	200.0	2.5	
20 August 1944	Aeolian Islands	4		300.0		
18 April 1968	Liguria- Cote d'Azur	2	3.0			
12 July 1977	Southern Calabria		5.0			5.5 x10⁶ m³
20 April 1988	Aeolian Islands	2	1.0 - 2.0		5.5	0.2x10⁶ (subaerial)
30 December 2002	Aeolian Islands	5	0.75 - 10.0	5.0 - 134.0	1.5 - 10.9	20x10⁶ (submarine) 4-9x10⁶ (subaerial)

(b)

Table 3 Summary of data about tsunami simulated in the Western Mediterranean Region and affecting the Italian subregions

	Tsunami event	Source area	Main features of triggering mechanisms	Exposed zones	Tsunami amplitude	Reference
Earthquakes	11 January 1693	The earthquakes location is still matter of debates. An offshore epicentre located along the Hyblean-Malta escarpment has been assumed by [1], while other authors [3, 4] do not exclude the possible occurrence of a landslide close to the foot of the escarpment at about 30–35 km off Augusta	Mw = 7.4 Landslide volume = 4.8 km³ [4]	A strong seismic sequence, starting on 09 January 1693, hit the eastern Sicily. The main shock of 11 January razed to the ground Catania, Augusta, Noto and Siracusa cities. This event generated a tsunami that devastated the entire eastern Sicily coasts, damaged the Malta archipelago and was observed in a large portion of the western Ionian Sea. After 45 min the entire Ionian coast of Calabria was also hit. After 1 h the tsunami reached the Southern Italy, Malta, southern Albania, Western Greece and Southern Peloponnesus. Minor effects were also estimated in the Southern Adriatic Sea, the Sidra Gulf in Libya, the Egyptian coasts, and some limited coastal zones in the eastern Mediterranean basin. The maximum tsunami amplitude was 1 m [2]. For detail see online Appendix 1. Argnani et al. (2012) highlighted that considering the earthquakes as triggering mechanism, in about 10 min, the eastern Sicily and southern Calabria coasts were reached by a tsunami. A tsunami amplitude larger than 4 m was recorded in Catania and north of Siracusa, while the coast close to the Augusta village was impacted by a tsunami amplitude of about 10 m. In contrast the landslide is not able to produce waters larger than 1 m	No significant tsunami propagation in the Tyrrhenian Sea	[1] Tinti and Armigliato (2003; see references therein) [2] Tinti et al. (2005) [3] Tonini et al. (2011) [4] Argnani et al. (2012)

Table 3 continued

Tsunami event	Source area	Main features of triggering mechanisms	Exposed zones	Tsunami amplitude	Reference
23 February 1887	Offshore of Imperia, northern Italy	Mw = 6.9	The tsunami waters affected the coast from Marseille (France) to Livorno (Italy). Several simulations were performed but the S6 and S7 best fit with the earthquakes of 1887. In detail the scenarios S6 indicated a maximum tsunami amplitude of 3.2, 2.30 and 1.60 at Imperia, San Remo and Diano Marina respectively. The scenario S7 provided a value of 2.6, 1.9 and 1.5 maximum tsunami amplitude for the same localities	Negligible for the Southern Tyrrhenian Sea	Ioualalen et al. (2014)
28 December 1908	Messina Straits The identification of source is still far from being understood. The Earthquake was considered as triggering mechanism from [1]. A very large landslide was invoked by [5] while a composite source was considered reasonable by [6]	Mw = 7.2	A strong earthquake damaged Messina and Reggio Calabria towns and many other villages. Several tsunamis were observed along all the eastern Sicily and the south-western Calabria. The most intense hit all the coast of the Straits and was also observed in Malta (more than 400 km far from the source) and in Napoli harbour (more than 350 km far from the source). Two simulation were realized by [3]. The first uses the earthquakes as triggering mechanism while the second a composite source. According to the first simulation, after 9 min the tsunami reached the area offshore Catania; the maximum water elevation characterized the Messina Straits but tsunami amplitude of about 2 m was also recorded in the Catania harbour. The simulation of tsunami triggered by composite source give results more comparable with those observed. In a few minutes, the coast of eastern Sicily and of south-western Calabria was reached by tsunami. The maximum water elevation was recorded in Catania (4 m)	Value: 20–40 cm [7]	[1] Tinti and Armigliato (2003) [3] Tonini et al. (2011) [5] Billi et al. (2008) [6] Favalli et al. (2009) [7] Tinti and Giuliani (1983)

Table 3 continued

Tsunami event	Source area	Main features of triggering mechanisms	Exposed zones	Tsunami amplitude	Reference
10 October 1980	Algeria-Tunisia offshore, El Asnam	Mw = 7.1	The tsunami hit the Sardinia coast, except its northwestern sector, with tsunami amplitude higher than 0.5 m, sometimes exceeding 1.5 m. The effects were almost negligible in Southern Italy (reached in about 30 min), apart from limited coastal sectors of the northern coasts of Cilento (350–400 km), the Salerno Gulf, and the Gulf of Napoli (maximum tsunami amplitude within the range ± 0.5 m). Similarly, the western coast of Sicily was affected by tsunami amplitude of about ± 0.5 m	Value: 0.5 m	Lorito et al. (2008)
5 March 1823	Southern Tyrrhenian	Mw = 6.2	The tsunami reached the northern Sicily in less than 10 min with tsunami amplitude > 0.5 m and the Southern Italy in about 30 min; here the tsunami amplitude did not exceed 0.2 m, as confirmed by the synthetic marigrams in Napoli, Vibo Valentia and Orosei	Value: 0.1 m	Lorito et al. (2008)
Several events	Alboran Ridge	Mw = 6.7–7.2	The tsunami reached the coasts of the Alboran Sea in about 30 min, the maximal tsunami amplitude on the coast were close to 1.5 m	No significant tsunami propagation in the Central Tyrrhenian Sea	Álvarez-Gómez et al. (2011)

Table 3 continued

	Tsunami event	Source area	Main features of triggering mechanisms	Exposed zones	Tsunami amplitude	Reference
Landslide	11.5 ka BP [8]	Northwestern Mediterranean Sea, Ebro margin	The volume of mass-failure was estimated in about 26 km³ [9] The headwall has a sinuous shape; it develops from west to east between 600 and 1230 m of water depth	The simulation implemented by [10] showed that after 10 min the tsunami reached the Balearic Islands with a tsunami amplitude higher than 10 m. After 20 min, waters higher than 5 m affected the northern coasts of Ibiza and high water also hit the coast of Mallorca. In about 40 min, the perturbation reached the coast of mainland Spain. Moreover, the coasts of Africa, Sardinia and Corsica are affected by a tsunami amplitude of 5–7 m in about 90 min	Negligible for the Tyrrhenian Sea	[8] Lastras et al. 2002 [9] Canals et al. 2000 [10] Zaniboni et al. (2014a)
	5 ka BP	Stromboli Volcano	Inferred volume = 0.52–0.95 km³	The whole island coast may have been struck by tsunami amplitude ranging 20–50 m. In the far field, Tinti et al. (2003b) evidenced that Panarea and Salina Islands could have been hit first by the tsunami and the Sicilian and Calabrian coasts, shortly after. The waters could have been smaller in Sicily than in Calabria, in fact the latter was possibly reached by tsunami amplitude ranging 4–6 m; the most affected area, however, could have been the Capo Vaticano promontory, where the simulation gives tsunami amplitude exceeding 10 m	Negligible for the Gulf of Napoli	Tinti et al. (2003b and reference therein)
	3–2.4 ka BP	Ischia Island, southern sector	Inferred volume = 1.5–3 km³	The entire costs of the Gulf of Napoli could have been struck by the tsunami waters in about 8–25 min; the city of Napoli could have been reached in 15 min, with a maximum water elevation of about 20 m	maximum tsunami amplitude about 20 m	Tinti et al. (2011)

Table 3 continued

Tsunami event	Source area	Main features of triggering mechanisms	Exposed zones	Tsunami amplitude	Reference
6 February 1783	Southern Calabria, Scilla locality.	Volume = 5×10^6 m³. The landslide was triggered by a seismic event of 5.8 M	After 5 min the water front has reached the north-east Sicily coast and it moves along the coast of Calabria and Sicily. After 10 min the water front approached Bagnara Calabra north of Scilla and entered in Messina Straits. The run-up ranges between 15 and 35 m in the area close to the tsunami source (Marina di Scilla, Marina San Gregorio and Chianalea). Southward, at Cannitello and Catona localities a run-up value of about 1 m and 6–8 m was recorded, respectively. Along the Sicily coast the higher value of run-up (25–40 m) characterized Punta del Faro while at Messina this factor ranged between 1–3 m. In the first 20 min, the maximum tsunami amplitude was higher than 10 m	Negligible for the Gulf of Napoli	Mazzanti and Bozzano (2011)
12 July 1977	Southern Calabria, Gioia Tauro	Volume about 5.5×10^6 m³	After around 1 min, the narrow strip of land enclosing the harbour was affected by a wave at least 2 m high; the tsunami propagates inside the harbour only after 2–3 min		Colantoni et al. (1992) Zaniboni et al. (2014b)

Table 3 continued

Tsunami event	Source area	Main features of triggering mechanisms	Exposed zones	Tsunami amplitude	Reference
16 October 1979	Ligurian Sea, Nice international airport	Two consecutive mass failures: volume $1 = 0.00219$ km^3 in shallow water Volume $2 = 0.0622$ km^3 at a mean depth of 800 m	The coastal zone from Antibes to Nice was reached in 2–5 min. For volume 1, the tsunami amplitude was about 1.6 m in the area close to Nice international airport. The maximum water elevation of 1,86 m was recorded at Antibe–La-Salis beach and of 2.47 m at Nice international airport. For volume 2, the tsunami amplitude was about 0.8 m in the area close to Antibes. The maximum water elevation of 2.48 m was recorded at Antibe- La-Salis beach and of 4.64 m in the area close to Nice international airport	Negligible for the Tyrrhenian Sea	Ioualalen et al. (2010)
30 December 2002	Stromboli Volcano, Sciara del Fuoco	Two consecutive mass failures Volume $1 = 20 \times 10^6$ m^3 submarine and a 7 min later subaerial landslide; Volume $2 = 4–9 \times 10^6$ m^3	The tsunami waters reached all the coasts of Stromboli Island within a few minutes and arrived in less than 5 min at the neighbouring island of Panarea, 20 km SSW of Stromboli. They were observed all over the Aeolian archipelago, at Ustica Island, along the northern Sicily and Calabria coasts and in Campania (from Scario to Marina di Casalvelino) about 140 km far from Stromboli. In Campania, the sea withdrew from few metres to several ten of metres in the different places and successively invaded the coastal zones with a maximum value of 60–70 m at Marina di Camerota (Maramai et al. 2005a)	Negligible for the Gulf of Napoli	Tinti et al. (2006a, b)

Table 3 continued

Tsunami event	Source area	Main features of triggering mechanisms	Exposed zones	Tsunami amplitude	Reference
Al-Borani landslide	Al-Borani Ridge, southern flanks	Volume of the mass-failure = about 1 km³; the submarine landslide could have been triggered by a seismic event	The tsunami may have reached the North Africa coast in about 10 min, with a maximum wave amplitude of about 1.7 m. The first sector of the Southern Iberian coast that could have been hit by the tsunami waters, might be Sacratif Cape, in about 22 min, with tsunami wave amplitude of 0.82 m. The coastal zone between Fuengirola and Malaga could be interested by a significant resonance effect of tsunami waters. In detail, Fuengirola and Malaga could be reached by a maximum tsunami wave amplitude close to 0.58 m (in about 43) and to 0.43 m (in about 48 min), respectively	Negligible for the Tyrrhenian Sea	Macias et al. (2015)
In perspective, hypothetical	Ischia Island, Monte Nuovo, [11] modelled a rockslide-debris avalanche	Inferred volume = 30 10⁶ m³	The tsunami might affect the norther coast of Ischia Island in about 45 min, with water elevation exceeding 8–10 m. Along the western shore of the island, in the area of Citara, south of Forio village, modelled water waters might exceed 10 m. After 10 min, the remaining coasts of Ischia and the western side of Procida Island could be impacted by 1–2 m tsunami amplitude. Tsunami would also propagate towards the north-west, approaching the coast of the Campanian Plain up to Castel Volturno with a positive 2–3 m front in about 15–20 min. In the southern direction the tsunami would be weaker; it could affect the Island of Capri with waters not exceeding 2 m high and the Gulf of Napoli and the Sorrento Peninsula at its south-eastern border, with tsunami amplitude of about 1 m	Value: 0–1 m	[11] Zaniboni et al. (2013)

Table 3 continued

Tsunami event	Source area	Main features of triggering mechanisms	Exposed zones	Tsunami amplitude	Reference
Volcanic eruption	Somma-Vesuvio Volcano	Lightest component of pyroclastic flows	Gulf of Napoli	Value: 0.4 m at Napoli city.	Tinti et al. (2003a)
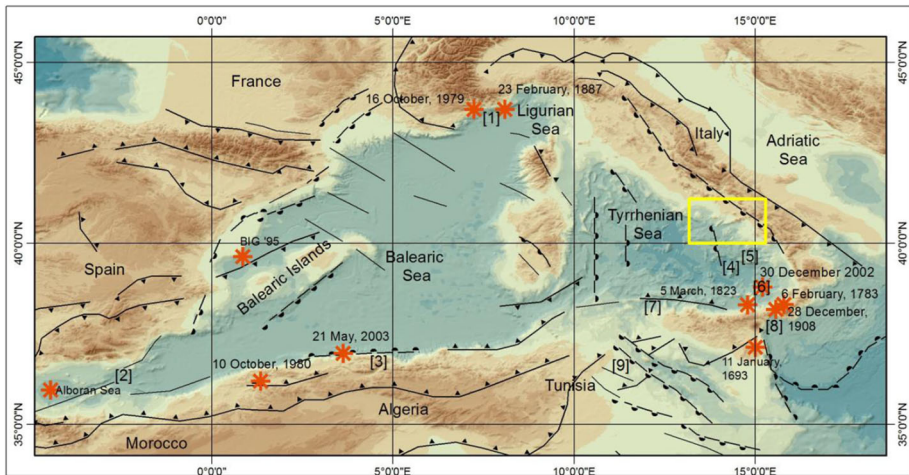
(a)
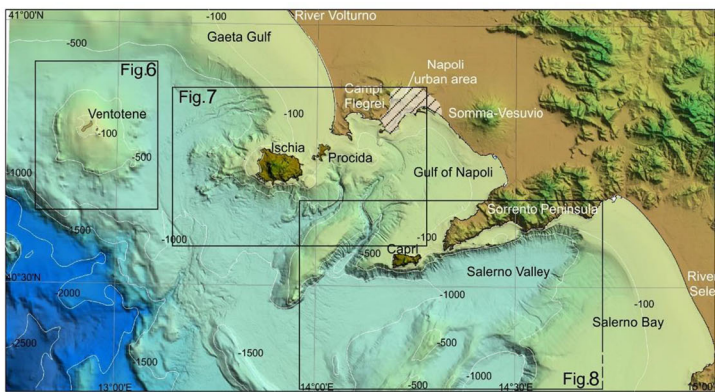
(b)

Fig. 5 **a** Topographic and bathymetric map of Western Mediterranean domain; the line symbols represent simplified geological structures (modified from Faccenna et al. 2003; Cavazza et al. 2004; Billi et al. 2011). The orange stars are the location of tsunami simulated in the Western Mediterranean Sea, while the numbers in the brackets indicate: 1-French Italian Riviera, 2-Alboran ridge, 3-Tell-Atlas thrust belt, 4-Marsili Seamount, 5-Palinuro Seamount, 6-Stromboli, 7-Southern Tyrrhenian thrust belt, 8-Messina Strait, 9-Hyblaean Malta escarpment. The yellow box indicates the location of study area illustrated in detail in the lower part of the image; **b** bathymetry off the Campania-Lazio regions, in the central Tyrrhenian Sea, by a composite swath bathymetric dataset of IAMC. Deep data from Emodnet, http://portal.emodnet-bathymetry.eu/

4.2 Tsunami generated by landslides

A large number of tsunamigenic landslides were generated in subaerial coastal settings or shallow marine areas, typically at the shelf edge or upper continental slope (Bondevik et al. 2005; Chaytor et al. 2007; Billi et al. 2008; Lo Iacono et al. 2011; Mazzanti and Bozzano 2011). For most of these events, it is still unclear if the tsunami was caused by co-seismic slip, by earthquake or by a combination of both mechanisms. In the Western Mediterranean, most failures have limited volume, short run-out and source in relatively deep water. Therefore, only the largest although infrequent events are likely to trigger large

tsunamis (e.g. Camerlenghi et al. 2010; Urgeles and Camerlenghi 2013). However, catastrophic sediment failures, such as the BIG'95 (11.500 cal year BP, the main features are summarized in Table 3) can also happen along continental margin not affected by significant earthquakes or active faulting (Lastras et al. 2002), such as those characterizing the northwestern Mediterranean Sea.

The propagation of a tsunami that may be triggered by a submarine landslide occurred on the southern flanks of the Alboran Ridge was simulated by Macias et al. (2015) (Table 3). They pointed out that shape and propagation patterns, wave amplitude and, finally, the area that may be exposed to this event (South Iberia and North Africa) are mainly influenced by the basin morphology.

Also in the Ligurian Sea, at the France–Italy border, numerous submarine landslides have occurred in the past along the narrow continental slope. The effects of the event occurred on 16 October 1979, simulated by Ioualalen et al. (2010), are summarized in Table 3. This event was divided into two main phases: the initial rupture at the shelf break involving a volume of 2.2×10^6 m^3 in shallow water; the ensuing phase of erosion and increasing volume occurred at about 800 m depth along the slope. The volume comparison has revealed that the moving slurry flow increased its volume 25 times in less than 3–4 km and in a short time period. A similar event had occurred 2 years before at the head of Gioia Canyon (Southern Tyrrhenian Sea), with a mobilized volume of 5.5×10^6 m^3, generating 5-m tsunami amplitude (Colantoni et al. 1992). More interestingly, in the surrounding area Casas et al. (2016), using high-resolution DEM, recognized several potentially tsunami-genic landslides occurring in shallow water.

Moreover, we also considered the inferred tsunamis which might have been triggered by landslides occurred in active volcanic area. In the last 13 ka BP, four coaxial flank collapses affected the NW flank of Stromboli volcano, the last one forming the Sciara del Fuoco (SdF) depression (Tibaldi 2001).The first of these collapses involved the Upper Vancori edifice about 13 ka BP (Tibaldi 2001) with an estimated volume exceeding 2×10^9 m^3, the second occurred in the early Holocene before 5.6 ka BP with a sliding mass in the order of 1×10^9 m^3 (Tibaldi 2001), the third more recent than 5 ka BP, involved a total volume of material of about 5.2×10^8–9.5×10^8 m^3 (Tibaldi 2001). The tsunami triggered by the last major slope failure was simulated by Tinti et al. (2003b), and the resulting characteristics are summarized in Table 3.

Marine studies recognized large debris avalanche deposits at the base both of the northwestern and eastern flank of Stromboli (Romagnoli et al. 2009a, b). The latter deposits on the E flank of Stromboli were attributed to (at least) two large sector collapses, the older one being comparable or larger in size to the collapses affecting the NW flank and the younger one (last few thousands of years) involving about 100×10^6 m^3 (Romagnoli et al. 2009b). Based on the mobilized volume and similar morphological setting with the NW flank, they have been considered responsible for the generation of large tsunamis comparable to those computed for the NW flank (Casalbore et al. 2011 and reference therein).

In more recent times, the tsunamis generated by a submarine and a 7 min later subaerial landslide (volume of approximately 10×10^6 m^3, and 4–9×10^6 m^3, respectively; Chiocci et al. 2008), affecting the NE part of the Sciara del Fuoco (December 2002), were investigated by Tinti et al. (2006a, b). It is noteworthy that similar events likely occur with high recurrence times (i.e. some tens of years) at the Sciara del Fuoco depression, as testified by the re-interpretation of five similar tsunami events which occurred in Stromboli in the past century (Maramai et al. 2005a) and by results of multi-lapse bathymetric

surveys to monitor the morphological evolution of the 2002 landslide scar (Chiocci et al. 2008).

Amongst the active volcanic seamounts located in the Tyrrhenian Sea, the steep slopes (25°–40°) of the Palinuro Seamount, coupled with the rock alteration and high fluid pressure, contribute to a slope instability often marked by mounded facies in the accumulation zone (Passaro et al. 2010 and reference therein). Similarly, the Marsili seamount showed signs of instability and eruptive or seismic events which might disrupt the unstable equilibrium of these rocks, intensely altered, generating mass failures (Ventura et al. 2013). Furthermore, Caratori Tonini et al. (2011) recognized a collapse in the western flank of the central-northern sector of Marsili seamount. The authors claim the threat associated with possible future mass failures in the area and the need of further investigations to assess the potential hazard.

4.3 Tsunami triggered by volcanic eruption

The Aeolian archipelago is an active volcanic area that should not pose significant hazard for the city of Napoli. Here, the tsunamis directly linked to volcanic activity have had only a local impact (Tinti et al. 2003a); as a matter of fact, only two tsunamis related to hot avalanche entering the sea occurred in the last 100 years; moreover, they only posed serious hazard only along the Aeolian Islands' coasts (Maramai et al. 2005b).

5 Tsunamis potentially generated at Napoli Gulf

5.1 Volcano-tectonic activity and tsunami events

In a volcanic area, earthquakes, rapid inflation or deflation of volcanic flanks, pyroclastic flows and lahars can occur during an eruption; the tight relationship amongst co-volcanic (or volcanic-induced) phenomena makes very difficult the identification of specific tsunami triggering factors. For the Napoli Gulf, a combined reading of historical documents, field data and simulation results is needed to solve the problem of scarcity of data relatively to the feedback between these events.

At present, the Somma-Vesuvio is characterized by a low level of seismicity (a few hundred micro earthquakes per year), with most of the earthquakes having a local magnitude (ML) < 3.0. The hypocenters are mainly located at very shallow depths (less than 5 km), and the strongest earthquake occurred in 9 October 1999 (ML 3.6) (Convertito and Zollo 2011).

At Campi Flegrei, the ground deformations are accompanied by low-energy shallow seismicity (Dvorak and Gasparini 1991). During the last bradyseismic episodes in 1969–1972 and 1982–1984, a maximum uplift of about 350 cm was observed and more than 16.000 local earthquakes were recorded. Seismicity was characterized by swarm-type activity; the largest event (MD = 4.2) occurred on 8 December 1984 (Del Pezzo et al. 1987). A ground uplift up to 4 cm occurred in March 2000 and was accompanied by two swarms of about 50 low-energy (MD ≤ 2.2) earthquakes occurred on 2–7 July, and 22 August 2000.

At Ischia Island seismic activity is concentrated in the northern part of the island around the town of Casamicciola and is characterized by a very shallow hypocentral distribution with typical depths between 1 and 3 km. Several events with maximum intensity I ≥ VII

MCS have occurred in the last few centuries (i.e. 1762, 1796, 1828, 1841, 1863, 1881 and 1883; Cubellis and Luongo 1998), causing landslides (Rapolla et al. 2010). Apart from the earthquake with intensity 6.2 MCS occurred on 22 August 2017, the island was characterized by low intensity seismicity over the last 130 years.

5.2 Analysis of tsunamis data and simulation results

The occurrence of anomalous waves has taken place not only during the largest explosive eruptions in the area (79 A.D., 1631) but also during low-size eruptive events (14 May 1698; 4 April 1906—Tinti and Maramai 1996) or prior to the beginning of volcanic activity (25 December 1813)—Lirer et al. 2009) (online Appendix 2). Moreover, a sea retreat was described for the eruption of 12 August 1804 (Scandone et al. 1993) and for the 1723 eruption (Lirer et al. 2009).

During the 1631 eruption, the contemporary accounts describe the occurrence of a tsunami reaching amplitude between 2 and 5 m in the Gulf of Napoli (online Appendix 2).

In his Geographica (source in Buchner 1986), the Greek writer Strabo (64 B.C.–21 A.D.) gives the description of a sudden collapse of a sector of the Ischia Island with an associated tsunami wave, dating prior to the Greek period, and recently dated between ∼ 3 and 2.4 ka BP (Ischia Debris Avalanche, IDA; de Alteriis et al. 2010). At Ischia Island, mass failures are, in fact, quite common (Della Seta et al. 2012); in many cases, they were caused by large-scale collapses of the over-steepened and faulted flanks of Mt. Epomeo resurgent block (Buchner 1986). The occurrence of these events is supported by large-scale slide scar recognizable onshore and facing coastal sector as well as by the local hummocky topography of the island offshore (Budillon et al. 2003; D'Argenio et al. 2004; Chiocci and de Alteriis 2006; de Alteriis and Violante 2009).

In a recent scientific work, the presence of tsunamis hazard triggered by the occurrence of debris avalanches at the Somma-Vesuvio volcano was inferred by Milia et al. (2012 and reference therein). They recognize two debris avalanches of about 1×10^9 m^3 (DA2), deposited in a time span very close to the Avellino eruption (4.2 ka BP—Santacroce et al. 2008), and of 3×10^9 m^3 (DA1), occurred during the Basal Pumice Plinian eruption (22 ka BP—Santacroce et al. 2008), respectively. They also recognize a submarine fan (volume: 3×10^8 m^3) interpreted as the result of the entry into the sea of AD 79 pyroclastic density currents.

The earthquake occurred in the Apennine Chain on 26 July 1805 (online Appendix 2) caused a rise of sea water in the Napoli Gulf (Poli 1806; D'Onofrio 1805; Baratta 1901).

Two tsunami simulations were performed for in the Napoli Gulf considering as triggering mechanisms the lightest component of pyroclastic flows as those occurred during large explosive eruptions of Somma-Vesuvio (Tinti et al. 2003a) and the Ischia Debris Avalanche (Tinti et al. 2011). Moreover, Zaniboni et al. (2013) have simulated a possible mass-failure event that might involve Monte Nuovo in response to a renewal of magmatic activity (Table 3).

5.3 Morphological-derived submarine mass failure parameters

The morphometric parameters of about 470 submarine landslide scars were measured between Ventotene Island (75 km to the NW of Napoli) and the northern sector of the Salerno Gulf (60 km to the SE) (Fig. 5b) in order to estimate the landslide-generated tsunami hazard from the marine sectors surrounding the city of Napoli. The landslide scars

below 700 m depth were excluded from the analysis for their intrinsic low hazard in relation to their size.

In the case of the Ventotene edifice, a total number of 126 landslide scars have been identified between − 130 and − 1150 m (Casalbore et al. 2014), with areas ranging from 0.1×10^6 to 10×10^6 m^2 (Fig. 6). The scars can be grouped into two types, one affecting the flanks of the edifice and the other occurring at the edges of the insular shelf, similarly to what was observed offshore other insular and oceanic islands (e.g. Romagnoli et al. 2013; Casalbore et al. 2015). However, none of these landslides was able to generate a maximum computed tsunami amplitude higher than 1 m. Taking into account the distance from the city of Napoli (ca. 75 km) and the inactivity of Ventotene edifice (last activity ended 0.15–0.3 Ma), the tsunami hazard related to landsliding processes affecting the submarine flanks of Ventotene edifice can be considered absent or very low for the Napoli city. Indeed, typical features of landslide-generated tsunamis are high amplitudes in the near-field and a rapid attenuation of the waves in the far field (Harbitz et al. 2006).

Around 350 landslides were identified along the continental margin between Volturno and the Sele river mouth. The greatest number of failures (up to 20/10 km^2) is observed north, west and south of the island of Ischia, a sector of the Campania continental margin largely controlled by volcanic features, such as cones, domes, dykes (Fig. 7). Landslide scars develop in water depth ranging between − 7 and − 900 m and occur in several morphological contexts: edge of submarine terraces, flanks of volcanic cones, canyon heads and walls, open slope, sedimentary aprons. Landslide scars are clustered around two modes: $0.20–0.4 \times 10^6$ m^2 and $0.6–2.0 \times 10^6$ m^2 wide, with volumes not exceeding 8×10^6 m^3 and $13–25 \times 10^6$ m^3, respectively. At least two failures, characterized by large volume and shallow coastal settings (− 35/− 240 m), resulted as potentially tsunamigenic with a computed maximum tsunami amplitude > 1 m. Differently, the large failure recognizable offshore the village of Casamicciola, at a water depth of about 7 m, partially remobilizing the northern debris avalanches, was not considered tsunamigenic, because it has been interpreted as a slow-moving slide by de Alteriis and Violante (2009).

A large number of landslides has been also observed at the headwalls and along the lateral walls of Magnaghi and Dohrn Canyons (D'Argenio et al. 2004; Milia 2000), in the depth range of 100–600 m. The instability processes have progressively enlarged the headwall of the Canyon Magnaghi through very small failures ($< 0.08 \times 10^6$ m^2). Differently, landslides in the canyon thalweg are at least one order of magnitude larger than the previous ones ($0.2–1 \times 10^6$ m^2). Several landslides ($0.5–1 \times 10^6$ m^2) have also been observed on the open slope between the canyon valleys (Fig. 7); they have a low potential hazard because located deeper than 200 m and characterized by volumes not exceeding 7×10^6 m^3. In this morphological context, few landslide scars larger than 1×10^6 m^2 were found at water depth shallower than − 300 m, implying a low potential tsunami hazard (Fig. 7).

The third group of submarine landslides runs along a Pleistocene structural lineament which bounds the southern side of the Sorrento Peninsula-Capri horst (Fig. 8) and controls the extension of the shelf edge (Milia and Torrente 1999; Casciello et al. 2006). The resulting 50-km-long escarpment is very steep (locally up to 20°) and an uneven seascape made of gullies, canyons, erosive scarps and aprons has developed through time. Locally, the emerged rocky cliffs are in continuity with the submerged slope and very small littoral wedges are preserved (Sacchi et al. 2009; Violante 2009). The greatest number (70%) of landslides is in shallow waters (< − 150 m) since the failures mostly occur along the shelf edge and account for a general retrogression of the continental slope. Despite the limited extension of the landslides, very high head scarps and very steep scar slopes have been
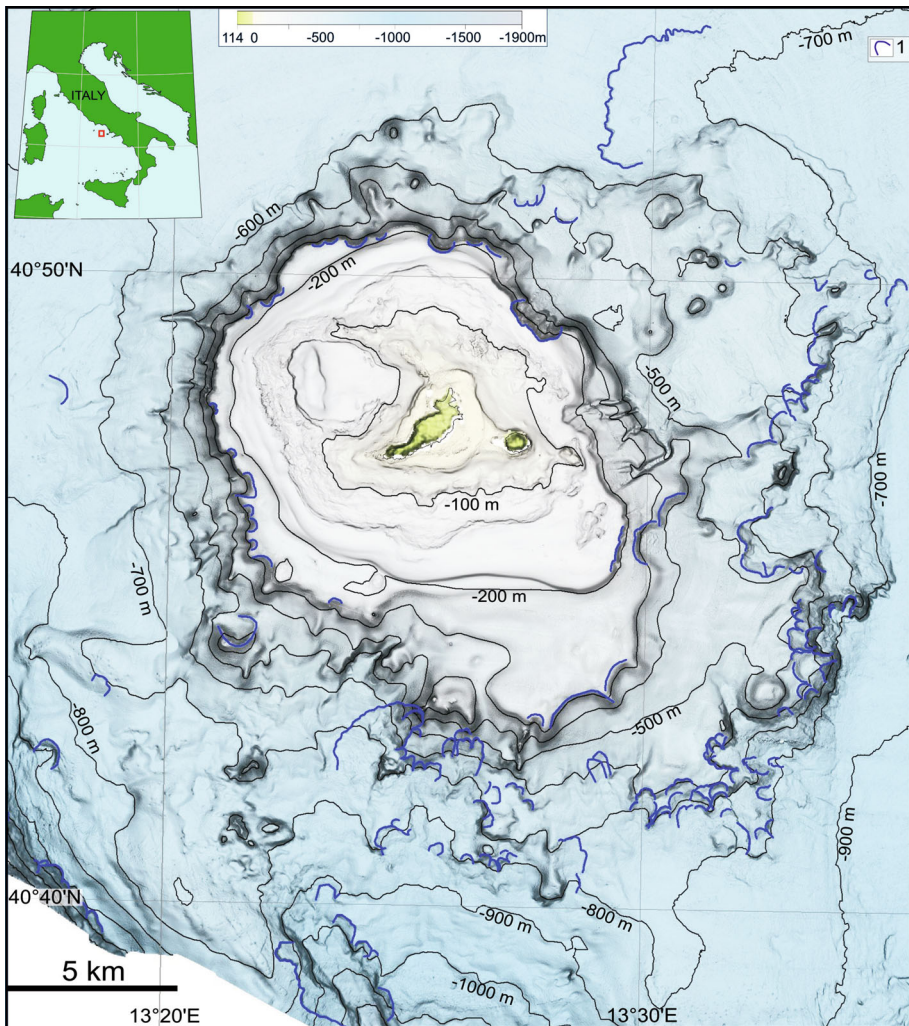
Fig. 6 Shaded relief map and isobaths (equidistance 100 m) of Ventotene edifice allow the recognition and morphometric characterization of 126 submarine scars (modified by Casalbore et al. 2014), based on the coupling between scar morphometry and predictive equations available in literature (see text for details); none of them resulted as being potentially tsunamigenic

observed. However, only two failures could have had a potential tsunami hazard, with computed maximum wave amplitude > 1 m high.

The southern edge of the Salerno Valley (Fig. 8) includes about 100 single failures, mostly distributed in 120–750 m depth range and a 14 km-long landslide complex, developed at 320–850 m water depth (Budillon et al. 2014). On the whole, they are translational landslides failed along weak layers with landslide scars characterized by several metres high head scarps and flat bottoms, corresponding to the slip surfaces. The largest single failure event identified in the area, which mobilized about 245×10^6 m^3 of material, is associated with a low tsunami hazard, due to the deep-water setting (> − 400 m).
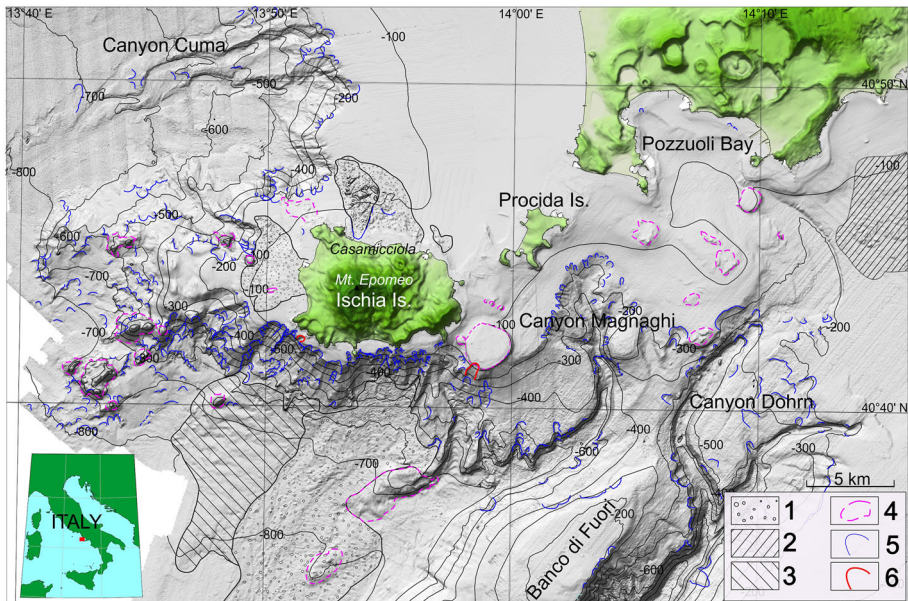
Fig. 7 Shaded relief map and isobaths (equidistance 100 m) of Ischia Island-Campi Flegrei offshore. The symbols indicate: (1) debris avalanches/debris flow deposit; (2) Banco della Montagna dome-like structure; (3) underwater creeping/slump deposit; (4) volcanic reliefs and banks (modified from Aiello et al. 2001; Milia and Torrente 2007; de Alteriis and Violante 2009; Della Seta et al. 2012); (5) non-tsunamigenic landslide (*maximum tsunami wave amplitude* < 1 m); 6) potentially tsunamigenic landslide (*maximum tsunami wave amplitude* > 1 m)

The morphometric analysis of mass failures in the near field pointed out that only four submarine landslides, with volume ranging from ca. 2.0 to 10.5 Mm^3 (Table 4) and occurring in relatively shallow water (15–360 m), could be considered potentially tsunamigenic, as their computed maximum wave amplitude (*A*) is encompassed between 1.18 and 1.71 m. This finding agrees with the recent observation that small and medium scale landslides (volumes up to tens of millions of cubic metres) in shallow waters can create local but sometimes destructive tsunamis, as for instance observed at Gioia Tauro in 1977 (Colantoni et al. 1992), Nice in 1979 (Sultan et al. 2010) and Stromboli in 2002 (Chiocci et al. 2008).

A proper modelling of landslide-generated tsunami propagation is beyond the aim of this paper, however, a first estimation of tsunami amplitude at the coast can be roughly made by applying the empirical relation between depth and amplitude of tsunami waves offshore (above the landslide scar) and in coastal sector (at − 1 m) provided by Federici et al. (2006). In the study area, the shoaling factor for the computed tsunami amplitude above the slide should be roughly comprised between 2 and 4.

6 Tsunami events

The identification of tsunami events possibly affecting the city of Napoli required the analysis of tsunamis occurred not only in the homonymous Gulf (near field) but also in all the Italian subregions. This paramount vision aimed to improve the knowledge on the
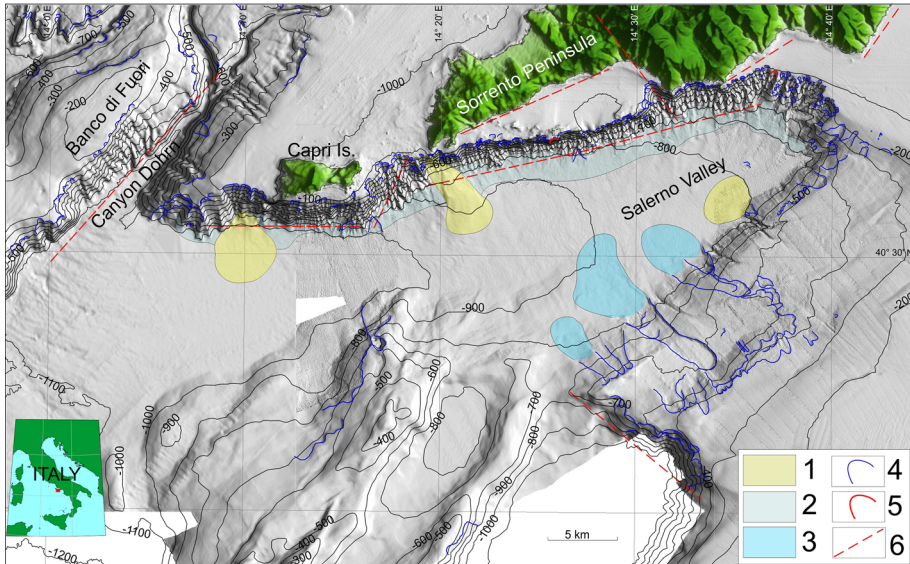
Fig. 8 Shaded relief map and isobaths (equidistance 100 m) of Capri Island-Sorrento Peninsula offshore. The symbols indicate: (1) deep sedimentary fan; (2) base of slope apron; (3) mass-wasting deposit (modified from Violante 2009; Budillon et al. 2014); (4) non-tsunamigenic landslide (*maximum tsunami wave amplitude* < 1 m); (5) potentially tsunamigenic landslide (*maximum tsunami wave amplitude* > 1 m); main fault. (modified from Milia and Torrente 1999; Casciello et al. 2006; Violante 2009)

events possibly affecting the city overcoming the paucity of quantitative data typical of a non-conservative environment as the volcanic areas. Moreover, the results of tsunami simulations realized in the Western Mediterranean Sea have been also considered.

The analysis of tsunami data concerning the Italian subregions and the simulations realized in the Western Mediterranean Sea highlighted:

- the main tsunami triggering causes for the Italian Peninsula are the earthquakes and volcanic eruptions with 54 (index value = 75%) and 10 (index value = 9%) events out of 72, respectively. The Campania (index value = 13.89%), Aeolian Islands and Tyrrhenian Calabria (index value: 11.11%) are the subregions more exposed to these events.
- The earthquakes magnitude index pointed out that 38 tsunami events out of 54 (index value = 70%) were generated by seismic events ≥ 5 Mw.
- Only 14 tsunamis out of 72 showed an intensity > 3 Mw (rather strong, according to Ambraseys 1962); in detail, these events were mostly triggered by earthquakes (sum of intensity index = 13.89), followed by volcanic eruptions (intensity index = 2.78), earthquakes and landslide (intensity index = 1.39) and eruption and landslide classes (intensity index = 1.39).
- The summary of tsunamis features evidenced a tsunami amplitude ≤ 4 m in 14 sites; higher values characterized tsunami events sourcing at Aeolian Island, Eastern Sicily, Messina Straits and Tyrrhenian Calabria and recorded in only seven sites (for detail see online Appendix 1). For the run-up and inland inundation tsunami features, a general rule could not be found since the local topography influenced the tsunami propagation. Moreover, the greatest part of sites reached by tsunami waves were characterized by an

Table 4 Morphometric parameters measured for the four potential tsunamigenic landslide recognized in the study areas (red lines in Figs. 7, 8)

ID	Sector	Scar minimum depth (m)	Barycentre depth (m)	Head scarp height (m)	Width (m)	Length (m)	Scar slope (°)	Volume (Mm^3)
5295d	Ischia Island, south-western offshore	33	100	27	390	380	23	2.0
5282	Ischia Island, south-eastern offshore	50	125	38	480	856	10	7.8
93	Sorrento Peninsula, southern offshore	170	280	60	660	530	21	10.5
123a	Sorrento Peninsula, southern offshore	98	360	125	500	200	40	6.2

inland inundation lower than 200 m, only in five localities this value was overcome (Table 2a). These places were exposed to tsunami events occurred on the 22 May 1919 and 20 August 1944 at Aeolian Island, on the 6 February 1783 at Scilla (Messinia Straits) and on the 28 December 1908 in the Messinia Straits (for detail see Appendix 1).

- The analysis of tsunamis simulation triggered by earthquakes (magnitude: from 6.2 to 7.4 Mw) sourcing in Southern Tyrrhenian and along the coasts of Algeria and Tunisia might generate tsunami amplitude ranging from 0.1 to 0.5 m in the Gulf of Napoli.
- Volcanic eruptions occurred in the far field, as those characterizing the Aeolian Islands and Etna Volcano, have had only local effects (Table 3).
- Landslides, with a volume ranging from few to several millions cubic metres, occurring in several sites of Mediterranean Sea did not propagate in the Gulf of Napoli (Table 3).

For the near field, the analysis of data pointed out a tsunami hazard mainly related to the Neapolitan volcanoes activity. The tsunami data analysis concerning the event occurred or simulated in the near field highlighted:

- tsunamis with low intensity (value = 2) could be triggered by volcanic eruptions. The tsunami amplitude ranges from centimetres to a few metres. In detail, during the Somma-Vesuvio eruptions, a tsunami amplitude of 30–40 cm was recorded for the 1906 eruption and of 2–5 m for the 1631 eruptions; a value of 1.8–2.7 m was reported for the earthquake of 1805 (online Appendix 2).
- The analysis of numerical simulations of tsunami events (Table 4) allowed to estimate a tsunami amplitude of about 20 m close to the coast of Napoli city linked to the debris avalanche occurred at Ischia Island (3 and 2.4 ka BP, de Alteriis et al. 2010) and of 0.4 m due to the propagation in the sea of the lightest component of pyroclastic flows sourcing at Somma-Vesuvio.

- The morphometric analysis of submarine landslide scars along the continental margin nearby the city of Napoli has evidenced that only 4 out of over 450 were potential tsunamigenic landslides. They could have generated tsunami amplitude of a few metres in the city of Napoli. Because of the steep gradients and concomitant presence of multiple predisposing and triggering factors for the development of instability processes along the Campania continental margin off Napoli, the possibility of future submarine landslides with size similar to the previous ones cannot be neglected.

7 Conclusive remarks

The integration of tsunami data for the events occurred in both near (from Ventotene Island to the northern sector of Salerno Gulf) and far (from other Italian subregions and Western Mediterranean Sea) fields made possible to identify the main source areas of tsunami events which might affect the city of Napoli in the future. Concerning the tsunamis generated by earthquakes in the far field (Western Mediterranean), only those triggered by high magnitude events (value $\geq$ 6–7 Mw) might affect the city of Napoli in about 30′; however, the expected maximum tsunami amplitude would not exceed 0.5 m, according to the analysed data.

Concerning the landslide-generated tsunamis, those sourced in the far field are far to represent a serious hazardousness for the city of Napoli, if the recurrent instability of Stromboli Island is excluded. As its instability is concerned, mass failures with volumes higher than those occurred in December 2002 (e.g. the sector collapse at 5 ka BP) could represent a potential hazard for the study area.

Concerning the landslide-generated tsunamis in the near field, the most critical source area could be represented by the southern submarine slope of Ischia and Sorrento peninsula where, in a recent past (20 ka BP), four landslides have occurred with a size and depth that could potentially trigger tsunamis with a maximum wave amplitude between 1.18 and 1.71 m. In addition, a possible sector collapse is thought to be occurred at Ischia in historical time, promoting the generation of tsunami waves up to 20 m high.

The hypothetical occurrence of a failure involving the Monte Nuovo at Ischia Island as much as the propagation of lightest components of pyroclastic flows emitted from the Somma-Vesuvio volcano could reach the city within 10–20 min with a tsunami amplitude ranging from 0.4 to 1 m.

This research aims to support the drawing up of a territorial plan sensitive to all natural hazards impending on the investigated area. The tsunami hazard has to be considered in the process of multi-hazard assessment for a correct allocation of resources dedicated to the risk reduction. In this frame, this work represents a first step towards the assessment of Neapolitan areas possibly exposed to tsunami inundation.

References

Aiello G, Budillon F, Cristofalo G, D'Argenio B, de Alteriis G, De Lauro M, Ferraro L, Marsella E, Pelosi N, Sacchi M, Tonielli R (2001) Marine geology and morphobathymetry in the Bay of Napoli (South-Eastern Tyrrhenian Sea, Italy). In: Faranda FM, Guglielmo L, Spezie G (eds) Structures and Processes of the Mediterranean Ecosystems. Springer-Verlag, Milan, pp 1–8

Alberico I, Petrosino P (2015) The hazard indices as a tool to support the territorial planning: the case study of Ischia Island (Southern Italy). Eng Geol 197:225–239

Álvarez-Gómez JA, Aniel-Quirogaa Í, Gonzáleza M, Olabarrietam M, Carreñod E (2011) Scenarios for earthquake-generated tsunamis on a complex tectonic area of diffuse deformation and low velocity: the Alboran Sea, Western Mediterranean. Mar Geol 284(1–4):55–73. https://doi.org/10.1016/j.margeo.2011.03.008

Ambraseys NN (1962) Data for the investigation of the seismic sea-waves in the Eastern Mediterranean. B Seismol Soc Am 52(4):895–913

Argnani A, Armigliato A, Pagnoni G, Zaniboni F, Tinti S, Bonazzi C (2012) Active tectonics along the submarine slope of south-eastern Sicily and the source of the 11 January 1693 earthquake and tsunami. Nat Hazards Earth Syst Sci 12:1311–1319. https://doi.org/10.5194/nhess-12-1311-2012

Baratta M (1897) Il Vesuvio e le sue eruzioni. Dall'anno 79 d.C. al 1896. Roma, Italy

Baratta M (1901) I terremoti d'Italia: saggio di storia, geografia e bibliografia sismica italiana (No. 9). Torino, Italy

Baratta M (1910) La catastrofe sismica Calabro messinese (28 dicembre 1908). Società geografica italiana, Roma

Bedosti B, Caputo M (1986) Primo aggiornamento del catalogo dei maremoti delle coste italiane. Atti della Accademia Nazionale dei Lincei. Classe di Scienze Fisiche, Matematiche e Naturali. Rend Lincei Mat Appl 80(7–12):570–584

Billi A, Funiciello R, Minelli L, Faccenna C, Neri G, Orecchio B, Presti D (2008) On the cause of the 1908 Messina tsunami, southern Italy. Geophys Res Lett 35(6):1–5. https://doi.org/10.1029/2008GL033251

Billi A, Minelli L, Orecchio B, Presti D (2010) Constraints to the cause of three Historical tsunamis (1908, 1783, and 1693) in the Messina Straits Region, Sicily, Southern Italy. Seismol Res Lett 81(6):907–915. https://doi.org/10.1785/gssrl.81.6.907

Billi A, Faccenna C, Bellier O, Minelli L, Neri G, Piromallo C, Scrocca D, Serpelloni E (2011) Recent tectonic reorganization of the Nubia-Eurasia convergent boundary heading for the closure of the western Mediterranean. Bull Soc Géol France 182(4):279–303

Bohannon RG, Gardner JV (2004) Submarine landslides of San Pedro Escarpment, southwest of Long Beach, California. Mar Geol 203(3–4):261–268. https://doi.org/10.1016/S0025-3227(03)00309-8

Bondevik S, Løvholtb F, Harbitzb C, Mangerudc J, Dawsond A, Svendsenc JI (2005) The Storegga Slide tsunami—comparing field observations with numerical simulations. Mar Pet Geol 22(1):195–208. https://doi.org/10.1016/j.marpetgeo.2004.10.003

Buchner G (1986) Eruzioni vulcaniche e fenomeni vulcanotettonici di età preistorica e storica nell'isola d'Ischia. In: Centre Jean Bérard, Institut Français de Napoli (ed) Tremblements de terre, eruptions volcaniques et vie des hommes dans la Campanie antique 7, pp 145–188

Budillon F, Violante C, De Lauro M (2003) I fondali delle Isole Flegree, morfologia e geologia. In: Gambi MC, De Lauro M, Jannuzzi F (eds) Ambiente marino costiero e territorio delle Isole Flegree (Ischia, Procida e Vivara—Golfo di Napoli). Risultati di uno studio multidisciplinare. Mem Acc Sc Fis Mat. Napoli, vol 5, pp 45–66. ISBN88-207-3557-1

Budillon F, Aiello G, Conforti A, D'Argenio B, Ferraro L, Marsella E, Monti L, Pelosi N, Tonielli R (2011a) The coastal depositional systems along the Campania continental margin (Italy, Southern Tyrrhenian Sea) since the Late Pleistocene: New Information Gathered in the Frame of the CARG Project. In: Brugnoli E et al (eds) Marine Research at CNR, Chapter Marine Geology, pp 540–551. ISSN 2239-5172

Budillon F, Conforti A, Tonielli R, D'Argenio B, Marsella E (2011b) Morfobatimetria del Golfo di Pozzuoli. In: Lirer L (ed) I Campi Flegrei, Storia di un campo vulcanico. Quaderni dell'Accademia Pontaniana, vol 57, pp 105–120

Budillon F, Cesarano M, Conforti A, Pappone G, Di Martino G, Pelosi N (2014) Recurrent superficial sediment failure and deep gravitational deformation in a Pleistocene slope marine succession: the Poseidonia Slide (Salerno Bay, Tyrrhenian Sea). In: Krastel S et al (eds) Submarine mass movements and their consequences, vol 37. Springer, Berlin, pp 273–283. https://doi.org/10.1007/978-3-319-00972-8_24

Camerlenghi A, Urgeles R, Fantoni L (2010) A database on submarine landslides of the Mediterranean Sea. In: Mosher DC, Moscardelli L, Shipp RC, Chaytor JD, Baxter CDP, Lee HJ, Urgeles R (eds)

Submarine mass movements and their consequences, Advances in natural and technological hazards research, vol 28. Springer, Dordrecht, pp 503–513

Canals M, Casamor JL, Urgeles R, Lastras G, Masson D, Berne S, Alonso B, De Batist M (2000) The Ebro continental margin, Western Mediterranean Sea: interplay between canyon-channel systems and mass wasting processes. In: Nelson H, Weimer P(eds) GCS SEPM Foundation 20th Annual Conference, Houston Texas (USA), pp 152–174 (CD edition)

Caputo M, Faita G (1984) Primo catalogo dei maremoti delle coste italiane. Atti Accad Naz Lin 17:213–356

Casalbore D, Romagnoli C, Bosman A, Chiocci FL (2011) Potential tsunamigenic landslides at Stromboli Volcano (Italy): insight from marine DEM analysis. Geomorphology 126(1–2):42–50. https://doi.org/10.1016/j.geomorph.2010.10.026

Casalbore D, Bosman A, Martorelli E, Sposato A, Chiocci FL (2014) Mass wasting features on the submarine flanks of Ventotene volcanic edifice (Tyrrhenian Sea, Italy). Submarine mass movements and their consequences, advances in natural and technological hazards research, vol 37. Springer, Berlin, pp 285–293. https://doi.org/10.1007/978-3-319-00972-8_25

Casalbore D, Romagnoli C, Pimentel A, Quartau R, Casas D, Ercilla G, Hipolito A, Sposato A, Chiocci FL (2015) Volcanic, tectonic and mass-wasting processes offshore Terceira Island (Azores) revealed by high-resolution seafloor mapping. Bull Volcanol 77:24. https://doi.org/10.1007/s00445-015-0905-3

Casalbore D, Romagnoli C, Bosman A, Anzidei M, Chiocci FL (2017) Coastal hazard due to submarine canyons in active insular volcanoes: examples from Lipari Island (southern Tyrrhenian Sea). J Coast Conserv. https://doi.org/10.1007/s11852-017-0549-x

Casas D, Chiocci F, Casalbore D, Ercilla G, de Urbina JO (2016) Magnitude-frequency distribution of submarine landslides in the Gioia Basin (southern Tyrrhenian Sea). Geo Mar Lett 36(6):405–414. https://doi.org/10.1007/s00367-016-0458-2

Casciello E, Cesarano M, Pappone G (2006) Extensional detachment faulting on the Tyrrhenian margin of the southern Apennines contractional belt (Italy). J Geol Soc 163(4):617–629. https://doi.org/10.1144/0016-764905-054

Cavazza W, Roure F, Spakman W, Stampfli GM, Ziegler PA (2004) The Tansmed Atlas—the Mediterranean region from crust to mantle. Springer, Berlin, pp 1–141

Chaytor JD, Twichell DC, ten Brink US, Buczkowski BJ, Andrews BD (2007) Revisiting submarine mass movements along the U.S. Atlantic continental margin: implications for tsunami hazards. In: Lykousis V, Sakellariou D, Locat J (eds) Submarine mass movements and their consequences. Advances in natural and technological hazards research, vol 27. Springer, Berlin, pp 395–403

Chiocci FL, de Alteriis G (2006) The Ischia debris avalanche: first clear submarine evidence in the Mediterranean of a volcanic island prehistorical collapse. Terra Nova 18:202–209. https://doi.org/10.1111/j.1365-3121.2006.00680.x

Chiocci FL, Romagnoli C, Bosman A (2008) Morphologic resilience and depositional processes due to the rapid evolution of the submerged Sciara del Fuoco (Stromboli Island) after the December 2002 submarine slide and tsunami. Geomorphology 100(3–4):356–365. https://doi.org/10.1016/j.geomorph.2008.01.008

Colantoni P, Gennesseaux M, Vanney JR, Ulzega A, Melegari G, Trombetta A (1992) Processi dinamici del canyon sottomarino di Gioia Tauro (Mare Tirreno). GeoActa 54(2):199–213

Convertito V, Zollo A (2011) Assessment of pre-crisis and syn-crisis seismic hazard at Campi Flegrei and Mt. Vesuvius volcanoes, Campania, southern Italy. Bull Volcanol 73(6):767–783. https://doi.org/10.1007/s00445-011-0455-2

Cubellis E, Luongo G (1998) Sismicità storica dell'isola di Ischia. In: Il terremoto del 28 luglio 1883 a Casamiccia nell'isola di Ischia—"il contesto fisico". Monografia n.1—Servizio Sismico Nazionale. Istituto Poligrafico e Zecca dello Stato Roma, pp 49–57

D'Onofrio A (1805) Lettera ad un amico in provincia sul tremuto accaduto a 2 luglio e seguito dall'eruzione vesuviana del 12 agosto del corrente 1805. Napoli

Dall'Osso F, Dominey-Howes D, Moore C, Summerhayes S, Withycombe G (2014) The exposure of Sydney (Australia) to earthquake-generated tsunamis, storms and sea level rise: a probabilistic multi-hazard approach. Sci Rep 4(7401):1–11. https://doi.org/10.1038/srep07401

D'Argenio B, Angelino A, Aiello G, de Alteriis G, Milia A, Sacchi M, Tonielli R, Budillon F, Chiocci F, Conforti A, De Lauro M, Di Martino G, d'Isanto C, Esposito E, Ferraro L, Innangi S, Insinga D, Iorio M, Marsella E, Molisso F, Morra V, Passaro S, Pelosi N, Porfido S, Raspini A, Ruggieri S, Sarnacchiaro G, Terranova C, Vilardo G, Violante C (2004) Digital elevation model of the Naples bay and adjacent areas, eastern Tyrrhenian Sea. In: Paquaré G, Venturini C, Groppelli G (eds) Mapping geology in Italy, APAT, S.E.L.C.A., Firenze, pp 21–28

De Alteriis G, Violante C (2009) Catastrophic landslides off Ischia volcanic island (Italy) during prehistory. Geol Soc Lond Spec Publ 322:73–104. https://doi.org/10.1144/SP322.3

De Alteriis G, Insinga DD, Morabito S, Morra V, Chiocci FL, Terrasi F, Lubritto C, Di Benedetto C, Pazzanese M (2010) Age of submarine debris avalanches and tephrostratigraphy offshore Ischia Island, Tyrrhenian Sea, Italy. Mar Geol 278(1–4):1–18. https://doi.org/10.1016/j.margeo.2010.08.004

Del Pezzo E, De Natale G, Martini M, Zollo A (1987) Source parameters of microearthquakes at Phlegrean Fields (southern Italy) volcanic area. Phys Earth Planet 47:25–42

Della Seta M, Marotta E, Orsi G, de Vita S, Sansivero F, Fredi P (2012) Slope instability induced by volcano-tectonics as an additional source of hazard in active volcanic areas: the case of Ischia island (Italy). Bull Volcanol 74(1):79–106. https://doi.org/10.1007/s00445-011-0501-0

Dvorak JJ, Gasparini P (1991) History of earthquakes and vertical movement in Campi Flegrei Caldera, southern Italy: comparison of precursory events to the A.D. 1538 eruption of Monte Nuovo and activity since 1968. J Volcanol Geotherm Res 48:77–92

Eckert S, Jelinek R, Zeurg G, Krausmann E (2012) Remote sensing-based assessment of tsunami vulnerability and risk in Alexandria, Egypt. Appl Geogr 32:714–723. https://doi.org/10.1016/j.apgeog.2011.08.003

EMTC (2014) http://roma2.rm.ingv.it/en/facilities/data_bases/52/catalogue_of_the_euro-mediterranean_tsunamis. Accessed 28 Mar 2017

Faccenna C, Jolivet L, Piromallo C, Morelli A (2003) Subduction and the depth of convection in the Mediterranean mantle. J Geophys Res Solid Earth. https://doi.org/10.1029/2001JB001690

Federici B, Bacino F, Cosso T, Poggi P, Rebaudengo Landó L, Sguerso D (2006) Analisi del rischio tsunami applicata ad un tratto della costa Ligure. Geomat Workb 6:53–57

Fournier D'Albe EM (1979) Objective of volcanic monitoring and prediction. J Geol Soc 136:321–326

Glade T (2003) Landslide occurrence as a response to land use change: a review of evidence from New Zealand. CATENA 51:297–314

Goldfinger LE, Jiang L, Hopkinson SB, Stack MS, Jones JC (2000) Spatial regulation and activity modulation of plasmin by high affinity binding to the G domain of the α3 subunit of laminin-5. J Biol Chem 275(45):34887–34893. https://doi.org/10.1074/jbc.M006652200

González FI, Geist EL, Jaffe B, Kânoğlu U, Mofjeld H, Synolakis CE, Titov VV, Arcas D, Bellomo D, Carlton D, Horning T, Johnson J, Newman J, Parsons T, Peters R, Peterson C, Priest G, Venturato A, Weber J, Wong F, Yalciner A (2009) Probabilistic tsunami hazard assessment at Seaside, Oregon, for near- and far-field seismic sources. J Geophys Res 114:C11023. https://doi.org/10.10029/2008JC005132

Graziani L, Maramai A, Tinti S (2006) A revision of the 1783–1784 Calabrian (southern Italy) tsunamis. Nat Hazards Earth Syst Sci 6:1053–1060

Grezio A, Gasparini P, Marzocchi W, Patera A, Tinti S (2012) Tsunami risk assessments in Messina, Sicily, Italy. Nat Hazards Earth Syst Sci 12:151–163. https://doi.org/10.5194/nhess-12-151-2012

Grilli ST, Watts P (1999) Modeling of waves generated by a moving submerged body. Applications to underwater landslides. Eng Anal Bound Elem 23(8):645–656

Guidoboni E, Tinti S (1988) A review of the historical 1627 tsunami in the Southern Adriatic. Sci Tsunami Hazards 6:11–16

Harbitz CB, Lòvholt F, Pedersen G, Masson DG (2006) Mechanisms of tsunami generation by submarine landslides: a short review. Nor J Geol 86:255–264

Heidarzadeh M, Krastel S, Yalciner AC (2014) The state-of-the-art numerical tools for modeling landslide tsunamis: a short review. In: Kraste S, Beahrmann JH, Volker D, Stipp M et al (eds) Submarine mass movements and their consequences, Advances in natural and technological hazards research, vol 37. Springer, Berlin, pp 483–495. https://doi.org/10.1007/978-3-319-00972-843

Ioualalen M, Migeon S, Sardoux O (2010) Landslide tsunami vulnerability in the Ligurian Sea: case study of the 1979 October 16 Nice international airport submarine landslide and of identified geological mass failures. Geophys J Int 181:724–740. https://doi.org/10.1111/j.1365-246X.2010.04572.x

Ioualalen M, Larroque C, Scotti O, Daubord C (2014) Tsunami mapping related to local earthquakes on the French-Italian Riviera (Western Mediterranean). Pure Appl Geophys 171(7):1423–1443. https://doi.org/10.1007/s00024-013-0699-1

Lander JF, Whiteside LS, Lockridge PA (2003) Two decades of global tsunamis. Sci Tsunami Hazards 21(1):3

Lastras G, Canals M, Hughes-Clarke JE, Moreno A, De Batist M, Masson DG, Cochonat P (2002) Sea floor imagery from the BIG'95 debris flow, western Mediterranean. Geology 30(10):817–874

Lirer L, Petrosino P, Alberico I (2001) Hazard assessment at volcanic fields: the Campi Flegrei case history. J Volcanol Geotherm Res 112(1–4):53–73

Lirer L, Petrosino P, Munno R, Grimaldi M (2009) Vesuvius through history and science. Mondadori Electa, Napoli

Lirer L, Petrosino P, Alberico I (2010) Hazard and risk assessment in a complex multi-source volcanic area: the example of the Campania region, Italy. Bull Volcanol 72(4):411–429. https://doi.org/10.1007/s00445-009-0334-2

Lo Iacono C, Sulli A, Agata M, Lo Presti V, Pepe F, Catatlano R (2011) Submarine canyon morphologies in the Gulf of Palermo (Southern Tyrrhenian Sea) and possible implications for geo-hazard. Mar Geophys Res 32(1):127–138. https://doi.org/10.1007/s11001-011-9118-0

Locat J, Lee HJ, Locat P, Imran J (2004) Numerical analysis of the mobility of the Palos Verdes debris avalanche, California, and its implication for the generation of tsunamis. Mar Geol 203(3):269–280. https://doi.org/10.1016/S0025-3227(03)00310-4

Lorito S, Tiberti MM, Basili R, Piatanesi A, Valensise G (2008) Earthquake-generated tsunamis in the Mediterranean Sea: scenarios of potential threats to Southern Italy. J Geophys Res. https://doi.org/10.1029/2007JB004943

Løvholt F, Glimsdal S, Harbitz CB, Horspool N, Smebye H, de Bono A, Nadim F (2014) Global tsunami hazard and exposure due to large co-seismic slip. Int J Disaster Risk Reduct 10:406–418

Macias J, Vàzquez JT, Fernàndez-Salas LM, Gonzaàlez-Vida JM, Bàrcenas P, Castro MJ, Dìaz-del-Rìo V, Alonso B (2015) The Al-Borani submarine landslide and associated tsunami. A modelling approach. Mar Geol 361:79–95

Mallet R (1854) Catalogue of recorded Earthquakes 1606 B.C.–1850 A.D. Reports on the state of science, third report of the facts of earthquakes phenomena, British Association for the Advancement of Science, London, pp 1852–1854

Maramai A, Graziani L, Alessio G, Burrato P, Colini L, Cucci L, Nappi R, Nardi A, Vilardo G (2005a) Near-and far-field survey report of the 30 December 2002 Stromboli (Southern Italy) tsunami. Mar Geol 215:93–106. https://doi.org/10.1016/j.margeo.2004.11.009

Maramai A, Graziani L, Tinti S (2005b) Tsunamis in the Aeolian Islands (southern Italy): a review. Mar Geol 215(1):11–21

Maramai A, Brizuela B, Graziani L (2014) The Euro-Mediterranean Tsunami Catalogue. Ann Geophys-Italy 57(4):1–26

Mazzanti P, Bozzano F (2011) Revisiting the February 6th 1783 Scilla (Calabria, Italy) landslide and tsunami by numerical simulation. Mar Geophys Res 32(1–2):273–286. https://doi.org/10.1007/s11001-011-9117-1

McAdoo BG, Watts P (2004) Tsunami hazard from submarine landslides on the Oregon continental slope. Mar Geol 203(3–4):235–245. https://doi.org/10.1016/S0025-3227(03)00307-4

Mercalli G (1883) Vulcani e fenomeni vulcanici in Italia. In: Forni A (ed) Ristampa anastatica del 1981. Sala Bolognese, Milano, p 372

Milia A (2000) The Dohrn canyon: a response to the eustatic fall and tectonic uplift of the outer shelf along the eastern Tyrrhenian Sea margin, Italy. Geo Mar Lett 20(2):101–108. https://doi.org/10.1007/s003670000044

Milia A, Torrente MM (1999) Tectonics and stratigraphic architecture of a peri-Tyrrhenian half-graben (Bay of Naples, Italy). Tectonophysics 315(1999):301–318

Milia A, Torrente MM (2007) The influence of paleogeographic setting and crustal subsidence on the architecture of ignimbrites in the Bay of Naples (Italy). Earth Planet Sci Lett 263:192–206

Milia A, Torrente MM, Bellucci F (2012) A possible link between faulting, cryptodomes and lateral collapses at Vesuvius Volcano (Italy). Glob Planet Change 90–91:121–134. https://doi.org/10.1016/j.gloplacha.2011.09.011

Nakamura Y, Nishimura Y, Putra PS (2012) Local variation of inundation, sedimentary characteristics, and mineral assemblages of the 2011 Tohoku-oki tsunami on the Misawa coast, Aomori, Japan. Sediment Geol 282:216–277. https://doi.org/10.1016/j.sedgeo.2012.06.003

Nguyen PH, Bui QC, Vu PH, Pham TT (2014) Scenario-based tsunami hazard assessment for the coast of Vietnam from the Manila Trench source. Phys Earth Planet Inter 236:95–108. https://doi.org/10.1016/j.pepi.2014.07.003

NOAA (National Geographic Data Center). http://www.ngdc.noaa.gov/hazard/tsu_db.shtml. Accessed 29 Sept 2016

Omira R, Baptista MA, Miranda JM, Toto E, Catita C, Catalao J (2010) Tsunami vulnerability assessment of Casablanca—Morocco using numerical modeling and GIS tools. Nat Hazards 54(1):75–95. https://doi.org/10.1007/s11069-009-9454-4

Orfanogiannaki K, Papadopoulos GA (2004) Conditional probability approaches for the occurrence of earthquake generated tsunamis. Pure Appl Geophys 164:593–603. https://doi.org/10.1007/s0024-006-0170-7

Papathoma M, Dominey-Howes D (2003) Tsunami vulnerability assessment and its implications for coastal hazard analysis and disaster management planning, Gulf of Corinth, Greece. Nat Hazards Earth Syst Sci 3(6):733–747. https://doi.org/10.5194/nhess-3-733-2003

Passaro S, Milano G, D'Isanto C, Ruggieri S, Tonielli R, Po Bruno P, Sprovieri M, Marsella E (2010) DTM-based morphometry of the Palinuro seamount (Eastern Tyrrhenian Sea): geomorphological and volcanological implications. Geomorphology 115:129–140

Pesaresi M, Gerhardinger A, Haag F (2007) Rapid damage assessment of build-up structures using VHR Satellite Data in Tsunami Affected Area. Int J Remote Sens 28(13):3013–3036. https://doi.org/10.1080/01431160601094492

Platania G (1909a) Il maremoto dello Stretto di Messina del 28 dicembre 1908. Boll Soc Sism Ital 13:369–458

Platania G (1909b) I fenomeni marittimi che accompagnarono il terremoto di Messina del 28 dicembre 1908. Riv Geogr Italy 16:154–161

Poli GS (1806) Memoria sul tremuoto de' 26 luglio del corrente anno 1805. Napoli

Rahiman TI, Pettinga JR (2006) The offshore morpho-structure and tsunami sources of the Viti Levu Seismic Zone, southeast Viti Levu, Fiji. Mar Geol 232(3–4):203–225. https://doi.org/10.1016/j.margeo.2006.07.007

Rapolla A, Paoletti V, Secomandi M (2010) Seismically induced landslide susceptibility evaluation: application of a new procedure to the island of Ischia, Campania Region, Southern Italy. Eng Geol 114:10–25. https://doi.org/10.1016/j.enggeo.2010.03.006

Romagnoli C, Kokelaar P, Casalbore D, Chiocci FL (2009a) Lateral collapses and active sedimentary processes on the northwestern flank of Stromboli volcano, Italy. Mar Geol 265(3–4):101–119. https://doi.org/10.1016/j.margeo.2009.06.013

Romagnoli C, Casalbore D, Chiocci FL, Bosman A (2009b) Offshore evidence of large-scale lateral collapses on the eastern flank of Stromboli, Italy, due to structurally-controlled, bilateral flank instability. Mar Geol 262(1–4):1–13. https://doi.org/10.1016/j.margeo.2009.02.004

Romagnoli C, Casalbore D, Bosman A, Braga R, Chiocci FL (2013) Submarine structure of Vulcano volcano (Aeolian Islands) revealed by high-resolution bathymetry and seismo-acoustic data Marine. Geology 338:30–45

Sacchi M, Molisso F, Violante C, Esposito E, Insinga D, Lubritto C, Porfido S, Toth T (2009) Insights into flood-dominated fan-deltas: very high-resolution seismic examples off the Amalfi cliffed coasts, eastern Tyrrhenian Sea. Geol Soc Lond Spec Publ 322:33–71. https://doi.org/10.1144/SP322.2

Sahal A, Roger J, Allgeyer S, Lemaire B, Hébert H, Schindelé F, Lavigne F (2009) The tsunami triggered by the 21 May 2003 Boumerd'es-Zemmouri (Algeria) earthquake: field investigations on the French Mediterranean coast and tsunami modelling. Nat Hazards Earth Syst Sci 9:1823–1834

Santacroce R, Cioni R, Marianelli P, Sbrana A, Sulpizio R, Zanchetta G, Donahue DJ, Joron JL (2008) Age and whole rock-glass compositions of proximal pyroclastics from the major explosive eruptions of Somma-Vesuvius: a review as a tool for distal tephrostratigraphy. J Volcanol Geotherm Res 177:1–18

Scandone R, Giacomelli L, Gasparini P (1993) Mount Vesuvius: 2000 years of volcanological observations. J Volcanol Geotherm Res 58:5–25

SOER (2015) The European environment state and outlook Synthesis Report. Eur Environ Agency. https://doi.org/10.2800/944899

Sultan N, Savoye B, Jouet G, Leynaud D, Cochonat P, Henry P, Stegmann S, Kopf A (2010) Investigation of a possible submarine landslide at the Var delta front (Nice continental slope, southeast France). Can Geotech J 47(4):486–496

Szczucinski W, Chaimanee N, Niedzielski P, Rachlewicz G, Saisuttichai D, Tepsuwan T, Lorenc S, Siepak J (2006) Environmental and geological impacts of the 26 December 2004 Tsunami in coastal zone of Thailand—overview of short and long-term effects. Pol J Environ Stud 15(5):793–810

Tibaldi A (2001) Multiple sector collapses at Stromboli volcano, Italy: how they work. Bull Volcanol 63:112–125. https://doi.org/10.1007/s004450100129

Tinti S (1991a) Tsunami potential in southern Italy. Sci Tsunami Hazards 9(1):5–14

Tinti S (1991b) Assessment of tsunami hazard in the Italian Seas. Nat Hazards 4(2):267–283. https://doi.org/10.1007/BF00162792

Tinti S, Armigliato A (2003) The use of scenarios to evaluate tsunami impact in south Italy. Mar Geol 199(3–4):221–243. https://doi.org/10.1016/S0025-3227(03)00192-0

Tinti S, Gavagni I (1995) A smoothing algorithm to enhance finite-element tsunami modelling: an application to the 5 February 1783 Calabrian case, Italy. Nat Hazards 12:161–197. https://doi.org/10.1007/BF00613075

Tinti S, Giuliani D (1983) The Messina Straits tsunami of December 28, 1908: a critical review of experimental data and observations. Il Nuovo Cimento 6:429–442

Tinti S, Guidoboni E (1988) Revision of the tsunamis occurred in 1783 in Calabria and Sicily (Italy). Sci Tsunami Hazards 6:17–22

Tinti S, Maramai A (1996) Catalog of tsunami generated in Italy and in Cote d'Aruz, France a step towards a unified calalogue of tsunamis in Europe. Ann Geophys Italy 39(6):1253–1273

Tinti S, Bortolucci E, Armigliato A (1999a) Numerical simulation of the landslide-induced tsunami of 1988 on Vulcano Island, Italy. Bull Volcanol 61(1):121–137

Tinti S, Armigliato A, Bortolucci E, Piatanesi A (1999b) Identification of the source fault of the 1908 Messina earthquake through tsunami modelling. Is it a possible pask? Phys Chem Earth 24(5):417–421

Tinti S, Maramai A, Graziani L (2001) A new version of the European tsunami catalogue: updating and revision. Nat Hazard Earth Syst 1:255–262

Tinti S, Pagnoni G, Piatanesi A (2003a) Simulation of tsunamis induced by volcanic activity in the Gulf of Naples (Italy). Nat Hazards Earth Syst 5:311–320

Tinti S, Pagnoni G, Zaniboni F, Bortolucci E (2003b) Tsunami generation in Stromboli Island and impact on the south-east Tyrrhenian coasts. Nat Hazards Earth Syst Sci 3:299–309. https://doi.org/10.5194/nhess-3-299-2003

Tinti S, Maramai A, Graziani L (2004) The new catalogue of Italian tsunamis. Nat Hazards 33:439–465. https://doi.org/10.1023/B:NHAZ.0000048469.51059.65

Tinti S, Armigliato A, Pagnoni G, Zaniboni F (2005) Scenarios of giant tsunamis of tectonic origin in the Mediterranean. J Earthq Technol 464(42, 4):171–188

Tinti S, Pagnoni G, Zaniboni F (2006a) The landslides and tsunamis of the 30th of December 2002 in Stromboli analysed through numerical simulations. Bull Volcanol 68(5):462–479. https://doi.org/10.1007/s00445-005-0022-9

Tinti S, Maramai A, Armigliato A, Graziani L, Manucci A, Pagnoni G, Zaniboni F (2006b) Observations of physical effects from tsunamis of December 30, 2002 at Stromboli volcano, southern Italy. Bull Volcanol 68(5):450–461. https://doi.org/10.1007/s00445-005-0021-x

Tinti S, Maramai A, Graziani L (2007) The Italian tsunami catalogue – Version 2. http://portale.ingv.it/servizi-e-risorse/BD/catalogo-tsunami/catalogo-degli-tsunamiitaliani

Tinti S, Zaniboni F, Pagnoni G, Manucci A (2008) Stromboli Island (Italy): scenarios of tsunamis generated by submarine landslides. Pure Appl Geophys 165:2143–2167. https://doi.org/10.1007/s00024-008-0420-y

Tinti S, Armigliato A, Pagnoni G, Zaniboni F, Tonini R (2011) Tsunamis in the Euro-mediterranean region: emergency and long term countermeasures. In: Marine geo-hazards in the mediterranean, MONACO, CIESM, 2011, pp 113–120

Tonini R, Armigliato A, Pagnoni G, Zaniboni F, Tinti S (2011) Tsunami hazard for the city of Catania, eastern Sicily, Italy, assessed by means of Worst-case Credible Tsunami Scenario Analysis (WCTSA). Nat Hazards Earth Syst Sci 11(5):1217–1232. https://doi.org/10.5194/nhess-11-1217-2011

UNESCO (1972) Consultative meeting of experts on the statistical study of natural hazards and their consequences. France, Paris

Urgeles R, Camerlenghi A (2013) Submarine landslides of the Mediterranean Sea: trigger mechanisms, dynamics, and frequency-magnitude distribution. J Geophys Res 118(4):2600–2618. https://doi.org/10.1002/2013JF002720

Ventura G, Milano G, Passaro S, Sprovieri M (2013) The Marsili ridge (Southern Tyrrhenian Sea, Italy): an island-arc volcanic complex emplaced on a 'relict' back-arc basin. Earth Sci Rev 116(1):85–94

Violante C (2009) Rocky coast: geological constraints for hazard assessment. Geol Soc Lond Spec Publ 322:1–31. https://doi.org/10.1144/SP322.1

Ward SN (2001) Landslide tsunami. J Geophys Res Solid Earth 106(B6):11201–11215. https://doi.org/10.1029/2000JB900450

Watts P (2000) Tsunami features of solid block underwater landslides. J Waterw Port Coast Ocean Eng 126(3):144–152. https://doi.org/10.1061/(ASCE)0733-950X(2000)126:3(144)

Zaniboni F, Pagnoni G, Della Tinti S, Seta M, Fredi P, Marotta E, Orsi G (2013) The potential failure of Monte Nuovo at Ischia Island (Southern Italy): numerical assessment of a likely induced tsunami and its effects on a densely inhabited area. Bull Volcanol 75:763–776

Zaniboni F, Pagnoni G, Armigliato A, Tinti S, Iglesias O, Canals M (2014a) Numerical simulation of the BIG'95 Debris flow and of the generated tsunami. Eng Geol Soc Territ 4:97–102

Zaniboni F, Zaniboni F, Armigliato A, Elsen K, Pagnoni G, Tinti S (2014b) The 1977 Gioia Tauro Harbour (South Tyrrhenian Sea, Italy) landslide-tsunami: numerical simulation. Landslide Sci Safer Geoenviron 3:589–594. https://doi.org/10.1007/978-3-319-04996-0_90